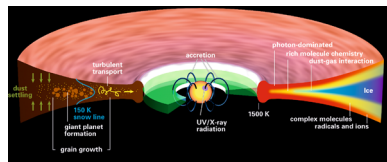


Chemistry in Protoplanetary Disks

Thomas Henning* and Dmitry Semenov*

Max Planck Institute for Astronomy, Königstuhl 17, D-69117 Heidelberg, Germany



CONTENTS

1. Introduction	9016
2. Physical Properties of Protoplanetary Disks	9018
2.1. Protoplanetary Disks as Accretion Disks	9018
2.2. Global Parameters of Protoplanetary Disks	9020
3. Material Inventory and Fundamental Chemical Processes in Disks	9021
3.1. Inventory of Gas-Phase Molecules	9021
3.1.1. Results from (Sub)millimeter Spectroscopy	9021
3.1.2. Results from Far-Infrared Spectroscopy	9021
3.1.3. Results from Mid- and Near-Infrared Spectroscopy	9022
3.2. Refractory Grains and Molecular Ices	9023
3.3. Main Chemical Processes	9024
3.4. Status of Chemical Models for Protoplanetary Disks	9028
3.5. Chemistry and Dynamics	9029
4. Water and Hydroxyl Molecules in Protoplanetary Disks	9030
5. Deuterium Chemistry in Disks	9032
6. Complex Organic Molecules	9033
7. Conclusions	9035
Author Information	9036
Corresponding Author	9036
Notes	9036
Biographies	9036
Acknowledgments	9036
References	9036

1. INTRODUCTION

Since the discovery of the first extrasolar planet around a solar-type star,¹ more than 900 such planets outside of our solar system have been detected by ground- and space-based astronomical observations.^{2–4} Even more planetary candidates discovered by the Kepler space mission await secure identification (<http://exoplanet.eu>). These exoplanets show a wide diversity in orbital parameters, ranging from close-in Hot Jupiters and Neptunes to planets on very eccentric orbits, in orbital resonances, and on retrograde orbits, and some located at very large distances from their host stars. A similar diversity has been found for the masses and radii of exoplanets, and initial investigations point to a diversity in the chemical composition and physical structure of their atmospheres.^{5–7}

The wide range of planetary system architectures and exoplanet properties is certainly linked to a range of properties of their birth-places, the disk-like structures around young stars composed of gas and dust particles.^{8–11} These disks share many of the properties of the solar nebula from which the Sun and our planetary system formed, although their masses, radial dimensions, and internal structures can be very different.¹² Protoplanetary disks form through the gravitational collapse of their parental molecular cloud cores in a process regulated by the balance of gravitational, magnetic, gas pressure, and rotational forces.¹³ After the dissipation of the protostellar envelope and the birth of a central star (central stars), the surrounding protoplanetary disk continues to regulate the inward radial transport of matter and the associated angular momentum transport outward, and, therefore, forms a special class of accretion disks.¹⁴

Thanks to the progress in infrared and radio astronomy starting in the early 1990s, and followed by highly successful infrared space observatories such as ISO, Spitzer, and Herschel, protoplanetary disks have been found and characterized in large numbers in regions of nearby star formation. They are discovered through their infrared and (sub)millimeter thermal dust emission being in excess of the radiation from the stellar photosphere of their central stars^{15,16} (for a review of their properties, see ref 12). Dust spectroscopy has revealed the mineralogical composition of the protoplanetary dust particles that are mostly found in the form of amorphous silicates, crystalline forsterite, water ice, and other molecular ices. There is strong observational evidence that the dust particles in disks can grow in size far beyond the typical sub-micrometer sizes of interstellar dust grains.¹⁷

In recent years, some of these disks have even been directly imaged with the Hubble Space Telescope, ground-based adaptive-optics assisted instruments (see Figure 1), and infrared and millimeter interferometry. The interferometry technique combines the light gathered by a number of telescopes to reach higher spatial resolution than available with the largest single-dish telescopes. These observations have revealed a wide diversity of protoplanetary disk structures, including some disks at advanced evolutionary phases showing inner holes or gaps devoid of emitting dust and sometimes even gas.^{19–22} These spatially resolved data confirmed the earlier inference of such structures based on the analysis of spectral energy distributions, especially provided by the Spitzer infrared space telescope.^{23–27} Other recent discoveries obtained with ground-based coronagraphic near-IR telescopes show large-scale, strong asymmetries in disk structure, such as spiral arms and density “knots”^{18,28,29}

Special Issue: 2013 Astrochemistry

Received: February 26, 2013

Published: November 5, 2013

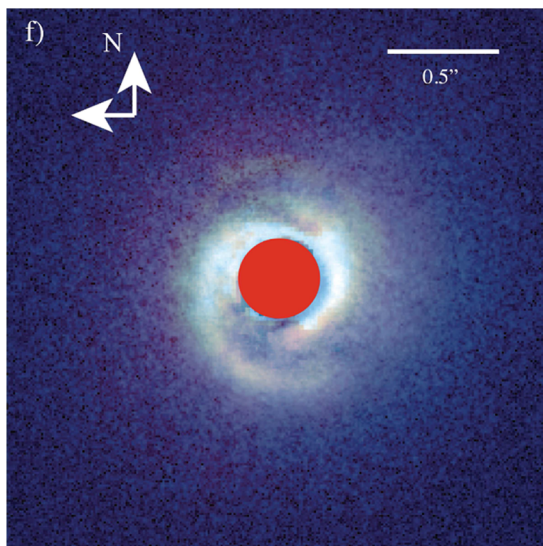


Figure 1. Near-IR scattered light image of the protoplanetary disk around the Herbig Ae star MWC 758 obtained with the Subaru telescope by the Strategic Exploration of Exoplanets and Disks (SEEDS) collaboration. Reprinted with permission from ref 18. Copyright 2013 American Astronomical Society.

(see Figure 1). These asymmetries are likely produced by a variety of physical processes such as magnetohydrodynamical turbulence,³⁰ grain growth beyond centimeter sizes,¹⁹ planet formation, and gravitational instabilities.³¹ These spatial structures immediately show that protoplanetary disks are not static systems, but are subject to strong dynamical changes on a time scale of several million years.¹²

The advent of sensitive infrared and (sub)millimeter spectroscopic observations enabled the discovery of thermal emission and scattered light from dust particles. In addition, a first inventory of atomic and molecular species has been provided, ranging from molecular hydrogen to water and more complex molecules such as polycyclic aromatic hydrocarbons (PAHs).^{32–34} At the same time, comprehensive chemical models for protoplanetary disks have been developed by a number of research groups (see Table 3), taking into account the wide range of radiation fields (UV and/or X-rays), temperatures (10 to several 1000 K), and hydrogen number densities (10^4 – 10^{12} cm⁻³). The combination of astronomical observations with advanced disk physical and chemical models has provided first constraints on the thermal structure and molecular composition of protoplanetary disks orbiting young stars of various temperatures and masses.^{35–39} These models have demonstrated that the chemistry in disks is mostly regulated by their temperature and density structure, and stellar and interstellar radiation fields as well as cosmic rays.^{40–49} A special feature of protoplanetary disks is the very low temperatures in the outer midplane regions, leading to a considerable freeze-out of molecules.^{50,51} At the same time, chemistry, together with grain evolution, regulates the ionization structure of disks,^{43,52–56} and, thereby, influences the magnetically driven transport of mass and angular momentum.⁵⁷ This means that disk chemistry and the physical structure of disks are ultimately linked. The impact of radial and/or vertical transport processes and dust evolution on disk chemical composition has been thoroughly theoretically investigated,^{54,58–68} and the predictions are being observationally confirmed.

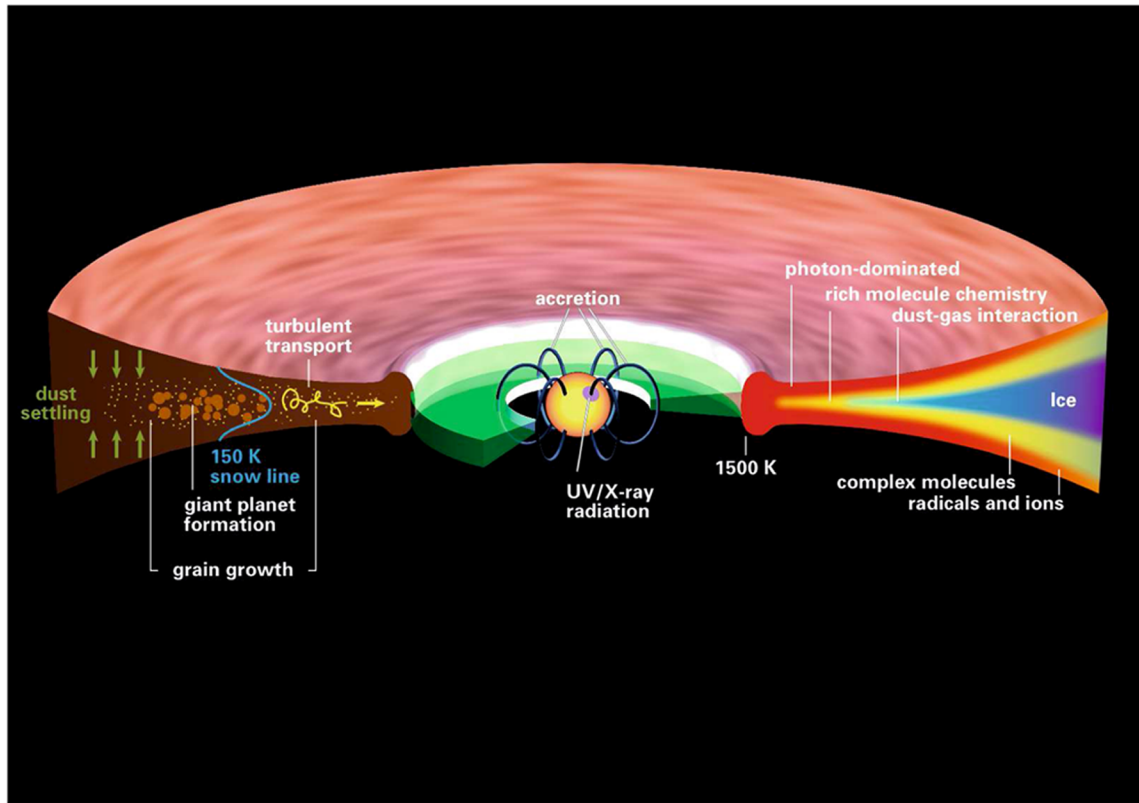


Figure 2. Sketch of the physical and chemical structure of a ~1–5 Myr old protoplanetary disk around a Sun-like star.

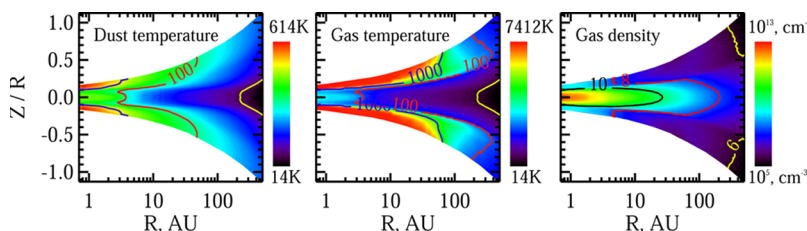


Figure 3. Vertical slice through a protoplanetary disk resembling the DM Tau system as calculated with the ANDES thermochemical disk model.⁷¹ The high values are marked by red color, and the low values are marked by dark blue/black colors. (Left) The radial and vertical profile of the dust temperature (in Kelvin). (Middle) The radial and vertical profile of the gas temperature (in Kelvin). Note that the gas temperatures are much higher than the dust temperatures in the disk surface layers. (Right) The radial and vertical profile of the gas particle density (in cm^{-3}).

With the Atacama Large Millimeter/Submillimeter Array (ALMA, <http://almascience.eso.org/about-alma/overview/alma-basics>) in Chile becoming fully operational and providing a giant step in sensitivity, spectral, and spatial resolution, and with models connecting planet formation with planet evolution, we can expect that protoplanetary disk chemistry will become a major topic in the rapidly evolving field of astrochemistry. This review will discuss these fascinating, chemically active places of planet formation and will summarize the information we have obtained about the physical structure and molecular chemistry of protoplanetary disks.

Because chemistry depends so much on temperature, density, and radiation fields in disks, and is influenced by disk dynamics, in section 2 we first provide a comprehensive description of the physics of protoplanetary disks. Section 3 summarizes the fundamental chemical processes in disks and presents an inventory of gas-phase molecules and ices. This review emphasizes the role of water in disks in section 4 because of its relevance for planet formation and the delivery of water to Earth. A special section 5 is devoted to deuterium fractionation in disks because this process may allow researchers to reconstruct the history of chemical and physical processes in early phases of the solar nebula and protoplanetary disks. The formation of complex organic molecules is the focus of section 6 because of its relevance for the delivery of organic materials to terrestrial planets.

2. PHYSICAL PROPERTIES OF PROTOPLANETARY DISKS

2.1. Protoplanetary Disks as Accretion Disks

Protoplanetary disks can be described as rotating dusty gaseous systems transporting a net amount of mass toward the central star and the angular momentum outward (see Figure 2). These disks are characterized by strong radial and vertical temperature and density gradients (see Figure 3). High-energy stellar and interstellar radiation may penetrate into the upper layers of disks, enabling a rich molecular chemistry. In the deep and well-shielded interiors temperatures become so low that molecules freeze out. The shielding is mostly provided by micrometer-sized solid dust particles. Apart from chemical evolution, the disks are characterized by strong evolution of the initially micrometer-sized dust particles toward pebbles and, finally, planets. This process has a strong impact on the physical structure of the disks, and therefore on the chemistry.

Protoplanetary disks are a special class of accretion disks. Accretion is a mass flow caused by the loss of potential energy due to frictional dissipation, which also leads to mechanical heating of the gas. The velocity, temperature, and density structure of accretion disks can be described by the

conservation equations for energy, mass, and momentum. For a geometrically thin disk, the time evolution of the surface density Σ can be expressed in the form of a nonlinear diffusion equation with the viscosity ν as the regulating parameter of the diffusion process.^{69,70}

The viscous stresses that are required for the evolution of accretion disks cannot be solely provided by the molecular viscosity of the gas, which is many orders of magnitude too small to have any considerable effect on mass and angular momentum transport. Instead, a “turbulent” viscosity has been invoked to explain the accretion behavior of protoplanetary disks. The origin of this viscosity was initially not known, and thus, it has been often conveniently parametrized by the so-called α parameter, $\nu = \alpha c_s H$, where c_s is the sound speed and H is the scale height of the disk.⁷² A quantity $\alpha \ll 1$ describes the regime of subsonic turbulence, $\alpha \sim 1$ – transonic turbulence, and $\alpha \gg 1$ – supersonic turbulence. Typical values for α inferred for protoplanetary disks range between 0.001 and 0.1.^{12,73,74}

In the case of steady-state optically thick disks with local energy dissipation the kinetic temperature T decreases with disk radius as $R^{-3/4}$. The mass accretion rate in such an α -disk is given by $dM(R)/dt \propto \nu \Sigma(R) \propto \alpha c_s(R) H(R) \Sigma(R)$, where $\Sigma(R)$ is the surface density (g cm^{-2}). The gas in disks moves on nearly circular orbits because the radial velocity component is much smaller than the angular velocity. In most cases the mass of the central star(s) exceeds by far the mass of the disk itself, and the angular velocity is given by the Kepler law, with $V_K = (GM_*/R)^{1/2}$ (where G is the gravitational constant and M_* is the mass of the central star). If one assumes that the disk is isothermal in vertical direction, then the ratio H/R should increase with radius R and the disk has a “flared” geometry.^{75,76}

The physical origin of the turbulent viscosity in accretion disks, especially in protoplanetary disks, is a major topic of ongoing astrophysical research. In ionized accretion disks a powerful magnetorotational instability (MRI) can efficiently drive angular momentum transport and provides effective α values of the right order of magnitude.^{57,73,77} However, in deep disk interiors, where even cosmic rays are not able to penetrate efficiently, the ionization degree drops to very low values, and dust grains become the dominant charge carriers.^{43,78,79} This can halt the MRI locally and thus results in a turbulent-inactive region (where α -values drop well below 0.01).

These dynamically quiet “dead” zones together with the more turbulent disk regions can result in very complicated density, temperature, and velocity structures in protoplanetary disks.^{30,80,81} In very massive disks and/or the colder outer regions of disks global gravitational instabilities can occur, which are another potential source of angular momentum transport. The effective operation of gravitational instabilities

depends strongly on the delicate balance between local cooling and heating rates, which are often difficult to constrain.^{82,83}

The thermal structure of protoplanetary disks, obviously a key parameter for disk chemistry, is not only determined by the dissipation of accretion energy. In fact, accretion heating is only dominant in the very inner, densest disk region where planets form, while in the inner surface layers and the outer disk regions the processing of stellar and interstellar radiation by dust particles plays a key role.^{84,85} The protoplanetary disks are divided on three different classes according to the luminosity and mass of their central stars: (1) disks around brown dwarfs, (2) disks around Sun-like T Tauri stars, and (3) disks around more luminous and massive Herbig Ae/Be stars.

Brown dwarfs are “failed” stars that are not massive enough to empower hydrogen burning, and which produce internal energy solely by gravitational contraction followed by slow, steady cooling. Not much is known yet with respect to chemistry in their disks, both theoretically and observationally, so we will not discuss it in our review. T Tauri stars are young, $\gtrsim 10$ Myr, pre-main sequence stars of the F–M spectral types, which are surrounded by gaseous nebulae. They have masses below $\sim 2M_{\text{Sun}}$, surface temperatures similar to that of the Sun, and large radii $\gtrsim 2R_{\text{Sun}}$. Hydrogen burning does not start in their interiors until they are about 100 million years old, so, like brown dwarfs, they are still powered by gravitational contraction. T Tauri stars are active and highly variable, with strong stellar winds, and intense thermal X-ray and nonthermal FUV radiation.^{86–88} Herbig Ae/Be stars are more massive ($\sim 2–8M_{\text{Sun}}$), hotter ($\sim 8000–15\,000$ K), and more luminous ($\gtrsim 15–200L_{\text{Sun}}$) counterparts to the T Tauri stars of the spectral types A or B.⁸⁹ Being hot, Herbig Ae/Be stars produce stronger thermal UV radiation than the T Tauri stars. Their X-ray luminosities are in general lower than those of the T Tauri stars due to the lack of efficient dynamo mechanism in their nonconvective photospheres.^{90,91}

In strongly accreting disks the midplane temperatures can be as high as 1000 K at radii of several AU.⁹² The direct irradiation from the central star can lead to the formation of inner disk walls, and thus disk shadows and complicated flaring patterns.⁹³ The highest dust temperatures in the disks, $T \sim 1500$ K, are set by the sublimation temperatures of the most refractory solids (e.g., corundum, Al_2O_3) and combustion-like destruction of carbonaceous compounds.⁹⁴ Apart from radial temperature gradients, we can also expect a steep rise of temperature in the vertical direction. All these factors make the construction of realistic disk models a challenge, and obviously, a multidimensional description is required.

In most current disk physical models the disk structure is considered to be in hydrostatic equilibrium between gravity and thermal pressure. Consequently, the vertical density distribution can be approximately described by a Gaussian function with $\exp(-(z/H)^2)$, where z is the vertical disk height. In the deeper interiors of the disks, dust and gas remain well-coupled through collisions, and the kinetic temperature of the gas is equal to the dust temperature. This is not the case in the upper tenuous disk layers, where a detailed balance of gas heating processes, mostly dominated by photoelectric heating by the stellar FUV radiation, and gas cooling through CO, C, C⁺, and O line emission and other cooling lines must be calculated.^{71,95–97} In disks where dust and gas are well-mixed, dust and gas temperatures are equal slightly above the optical depth = 1 surface.⁹⁵ This corresponds to gas particle densities of about $10^6–10^7 \text{ cm}^{-3}$.⁷¹ The exact density value for the dust–

gas coupling depends on the dust cross section per H atom. The collisional coupling between gas and dust may be reduced by dust settling to the midplane, decreasing the dust-to-gas ratio. In addition, grains may coagulate, which will also lead to a reduction of the dust cross section per hydrogen atom.^{71,97,98}

Photoelectric heating rates depend sensitively on the abundance of very small particles and polycyclic aromatic hydrocarbons (PAHs), which is often difficult to estimate.^{71,95,99} In addition to FUV radiation, strong X-ray emission and flares are observed in T Tauri stars, which is an important additional heating mechanism of the disk atmospheres by energetic secondary electrons.^{100,101} At a radial distance of 1 AU from the star, the gas temperature in the disk atmosphere can become as high as 5000–10 000 K (see Figure 3), which raises a question regarding the dynamical stability of this region. According to advanced disk models, it is plausible that the inner atmosphere is gradually lost, steadily reducing the disk mass and changing the global disk structure.^{45,48}

The gas accretion process is not the only driving force of disk evolution. Protoplanetary disks are also characterized by a variety of dust evolution processes, including dust growth, fragmentation, vertical sedimentation, and radial drift¹⁰² (for reviews see refs 17,103). The overall dust growth implies transformation of sub-micrometer-sized particles into kilometer-sized bodies, which covers many orders of magnitude on a spatial scale and which is governed by a multitude of physical processes. In essence, dust particles are assembled into centimeter-sized pebbles by Brownian motion, differential drift, and turbulence, followed by the dust decoupling from the gas and rain down of bigger grains toward the disk midplane. The headwind exerted on these pebbles by the gas that orbits at slightly sub-Keplerian velocity leads to rapid inward transport and loss of these pebbles (also due to mutual destructive collisions at $\gtrsim 10 \text{ m s}^{-1}$).^{102,104,105} Currently it is difficult to single out the most robust mechanism to overcome this so-called “1 m-size” barrier to continue the grain growth into the meter and kilometer regime. Plausible explanations include trapping of solids in turbulent eddies and other long-lived overdensities in disks produced by turbulence.^{105–108} When kilometer-sized bodies are formed from the pebbles, they interact with each other gravitationally, and efficient growth is regulated by the few most massive first planet embryos (“oligarchic” growth).

In the modern version of the so-called core-accretion scenario of planet formation,^{109–111} meter-sized rocks in the disk midplane become subject to gravitational instabilities leading to the formation of kilometer-sized planetesimals.¹¹² These planetesimals grow through gravitationally induced mutual collisions and coalescence to solid planet cores. Giant planets form if there is enough gas left in the disk to gravitationally collapse onto these cores, forming their massive atmospheres at the last stage of evolution. Upon formation, planets can further interact with the turbulent gas in disks and can radially migrate and clear gaps or entire inner holes, depending on the planet mass and the actual disk structure.¹¹³ An alternative scenario is the formation of massive clumps in outer cold regions of mostly massive protoplanetary disks.^{31,114} This scenario has recently again attracted attention in order to explain the presence of directly imaged massive planets or brown dwarfs on wide orbits.¹¹⁵ Detailed analysis of direct imaging data indicates that substellar companions formed by disk instabilities are rare, and the core accretion remains the

likely dominant formation mechanism for the entire planet population.¹¹⁶

2.2. Global Parameters of Protoplanetary Disks

The disks masses and sizes and their radial and vertical temperature and density distributions are important quantities both for the disk chemistry and the planet formation process. A comprehensive overview of how these quantities are actually measured through astronomical observations and which results have been obtained is provided by Williams and Cieza.¹² Here, we will only summarize some of the most important results.

The mass of protoplanetary disks is dominated by molecular hydrogen and helium in a mass ratio defined by the cosmic abundance of these elements. Unfortunately, the total disk masses cannot be determined directly from molecular hydrogen emission because H₂ is a homonuclear molecule without allowed electric dipole transitions and most of the disk mass is at temperatures too low to emit in ro-vibrational magnetic quadrupole transitions. These lines occur at near- and mid-infrared wavelengths and need excitation temperatures that are only provided in the very inner disk regions at several AU from the star [1 AU (astronomical unit) = mean distance between Sun and Earth]. Another complication is the fact that the emission from dust itself is often optically thick at these wavelengths and that one can only probe a very limited surface region of the disk.¹¹⁷ Disk emission from the CO molecule in its rotational transitions is frequently measured thanks to its relatively high abundance and permanent dipole moment. However, the CO/H₂ abundance ratio changes with radius and vertical depth because of three main factors. First, CO gas severely freezes-out on dust grains in the cold disk midplane (where temperatures drop below about 20 K).^{51,118} Second, in the irradiated disk atmosphere CO can be photodissociated by FUV radiation, despite the ability of this molecule to self-shield itself.^{44,46,119–121} Third, due to large concentrations of CO in disks, ¹²C¹⁶O rotational emission lines become saturated and probe the disk matter only at specific depths. The last problem can be circumvented by using rare isotopologue lines of CO having much lower optical depths, such as ¹²C¹⁸O and even ¹²C¹⁷O.¹²² This implies that mass estimates based on CO observations alone are highly uncertain, at least for the colder disks around T Tauri stars.

An elegant way to infer disk masses would be to use the rotational lines of HD to circumvent the H₂ and CO problem with disk mass determinations. However, this requires very high sensitivity at far-infrared wavelengths. The Herschel observatory provided the first such detection in the disk around the nearby star TW Hya.¹²³ This observation demonstrated that the disk mass in this system is not as small as previously thought and is at least 0.05M_{sun}.

The thermal emission of the dust particles can be relatively easily measured because of their much higher opacities. Under the assumption of optically thin disk emission, which is best fulfilled for protoplanetary disks at (sub)millimeter wavelengths, and with a specified dust opacity, which is often poorly constrained, the measured flux values can be directly converted into dust masses. The dust disk mass M_{dust} is given by

$$M_{\text{dust}} = F_{1.3\text{mm}} D^2 / \kappa(1.3\text{mm}) B_{1.3\text{mm}}(T_{\text{dust}}) \quad (1)$$

Here, F_{1.3mm} is the flux at 1.3 mm wavelength, D is the distance to the object, B_{1.3mm} is the Planck function at the dust temperature T_{dust}, and κ(1.3mm) is the mass absorption coefficient per gram of dust. One should note that the

measured dust emission is only sensitive to grain sizes up to millimeters and the mass reservoir in larger “boulders” cannot be constrained this way. Under the assumption of a canonical gas-to-dust mass ratio of 100, total disk masses can then be derived. With these caveats in mind, inferred median disk masses of 5 × 10⁻³ solar masses and a median disk-to-star mass ratio of 0.5% have been obtained from surveys of the Taurus-Auriga and ρ Ophiuchi star-forming regions.^{124–126} In a recent study¹²⁷ an inherently linear disk mass versus stellar mass scaling relation was found, but with a considerable dispersion at any given stellar mass, probably reflecting the combined effect of evolution, different dust properties, and temperatures. A considerable fraction of these disks has masses above 10 Jupiter masses, a minimum value of mass needed to form the solar system within the orbit of Neptune at ~30 AU. Other factors that influence the mass of disks through orbital interaction are close-in binaries or planetary systems. As stars rarely form in isolation, the proximity to very massive stars may lead to premature gas photoevaporation or disk disruption through dynamical interactions between cluster members.

Accretion rates in protoplanetary disks, mostly measured close to the star, cover a wide range of values from 10⁻⁹ to 10⁻¹²M_{sun} yr⁻¹. They depend on a variety of parameters, with the most important being the stellar mass^{128–130} and the stellar age and evolutionary status of the disk.^{23,131}

The disk radii are often difficult to determine precisely because of the vanishing emission at their cold and low-density outer edges. Submillimeter interferometric studies with high sensitivity and spatial resolution provided disk radii between 10 and 1000 AU (with a typical value of ~200 AU). An interesting observational finding has been that the sizes of the gas disks, as determined by CO emission, are significantly larger than the sizes of the dust continuum images.^{36,132} These studies also provided estimates for the radial surface density distribution, assuming a power law for regions not too close to the outer disk edge. Toward the outer disk edge radial surface density tends to fall off exponentially.¹²⁶ The obtained power law is relatively flat with a power law index close to -0.9.

The radial gas temperature distribution in the outer disk seems to follow a power law with a power law exponent between -0.4 and -0.7.^{36,133,134} These temperature distributions are similar to what has been obtained from the modeling of the continuum spectral energy distributions of disks.^{124,134}

Multiline studies in the low-lying rotational transitions (J = 1 – 0 up to 6 – 5) of CO isotopologues are presently providing a first insight in the vertical temperature structure of the outer regions of protoplanetary disks.^{36,135,136} These lines originate from different vertical layers of the disks depending on the location of the regions where their optical depths is close to 1. A rather surprising result of these studies was the discovery of a significant fraction of cold CO gas that has temperatures below the freeze-out temperature of CO of about 20 K.^{36,137}

Infrared surveys of large populations of disks in stellar clusters of various ages have shown that the disk frequency is a function of cluster age and steadily decreases from young star-forming regions with ages of 1 Myr to older regions of about 10 Myr¹³⁸ with a median disk lifetime of several Myr. Even shorter lifetimes were estimated for the presence of gas in inner disk regions, on the basis of measurements of the gas accretion rates.¹³¹ The search for colder gas in somewhat older systems has been largely unsuccessful with a few exceptions.¹³⁹ This implies that giant planet formation has to occur over the relatively short time scale of a few million years, much smaller

compared to the age of our solar system of 4.567 billion years, as measured by radioactive dating of various meteoritic samples.¹⁴⁰ Our present insight into the gas-phase composition of protoplanetary disks indicates that time scales of key chemical processes have to be shorter than ~ 1 Myr.⁶⁸

3. MATERIAL INVENTORY AND FUNDAMENTAL CHEMICAL PROCESSES IN DISKS

3.1. Inventory of Gas-Phase Molecules

The detection of molecular line emission at infrared wavelengths requires relatively high spectral resolution in order to isolate the weak molecular lines from the bright dust continuum emission of the disks. In addition, the protoplanetary dust disks are optically thick at infrared wavelengths, and line emission can only be observed from the tenuous warm surface layers. This is different for the (sub)millimeter wavelength range where the dust disks are optically thin and molecular line emission can be observed throughout the entire disk, although the inner dust disk may still be optically thick. We should note that the emission of many molecules originates from above the very cold midplane, where freeze-out of gaseous species onto grain surfaces occurs. The sensitivity and spatial resolution of the present (sub)millimeter facilities limits most of the observations to the very outer regions of disks beyond ≈ 30 – 100 AU and to the most massive disks around nearby objects such as TW Hya, DM Tau, and MWC 480. On the other hand, infrared spectroscopy can trace both molecular lines as well as characteristic absorption or emission features of solids. It is also sensitive to molecules without strong dipole moments, including PAHs with their forest of infrared emission lines. The different wavelength regimes correspond roughly to different temperatures and thus distinct disk regions, keeping in mind that the temperature is decreasing from the inner to the outer disk. We now discuss the results starting with the longest (sub)millimeter wavelengths and finishing with the near-infrared wavelengths.

3.1.1. Results from (Sub)millimeter Spectroscopy. (Sub)millimeter spectroscopy with single-dish and interferometric facilities has provided a first inventory of molecules in the outer regions of disks. Two major programs, “Chemistry in Disks” at the IRAM 30-m telescope and the Plateau de Bure Interferometer^{37,47,141–145} and “DISCS” at the SMA interferometer on Hawaii^{39,56,146} have provided most of the molecular line data on disk chemistry.

Apart from CO with its main isotopologues (^{13}CO and C^{18}O), a handful of relatively simple polyatomic molecules (HD, H_2CO , CS, C_2H , $\text{c-C}_3\text{H}_2$, HCN, HNC, CN, DCN) and molecular ions (N_2H^+ , HCO^+ , DCO^+ , H_2D^+) have been discovered by a variety of facilities. The various molecules trace different physical and chemical processes in the disks (see Table 1). The abundances of the discovered molecules relative to molecular hydrogen range between $\sim 10^{-10}$ and 10^{-4} . Here we note that astronomical observations provide line intensities, which have to be converted into column densities, assuming a specific temperature and density structure of the disk. This makes the analysis of molecular emission lines a challenging, nontrivial task, with resulting quantities usually uncertain by a factor of several.

Recently, the first heavier organic molecule, the cyanoacetylene HC_3N , was discovered in the disks around GO Tau and MWC 480.¹⁴⁴ Heavier polyatomic molecules remain undetected because of their low abundances, weak line intensities

Table 1. Molecular Lines as Tracers of Physical and Chemical Conditions in Disks

molecule	transitions	quantity	wavelengths
^{12}CO , ^{13}CO	rotational and ro-vibrational	temperature	IR, FIR, submm/mm
H_2	ro-vibrational	temperature	IR
$\text{CS}, \text{H}_2\text{CO}, \text{HC}_3\text{N}$	rotational	density	submm/mm
$\text{HCO}^+, \text{N}_2\text{H}^+, \text{CH}^+$	rotational	ionization	submm/mm, FIR
$\text{CN}, \text{HCN}, \text{HNC}$	rotational	photochemistry	submm/mm
$\text{H}_2\text{O}, \text{OH}$ (inner disk)	rotational	temperature	IR
$\text{H}_2\text{O}, \text{OH}$ (outer disk)	rotational	photochemistry photodesorption	FIR
complex organics (outer disk)	rotational	grain surface processes	submm/mm
complex organics (inner disk)	(ro-)vibrational	high- <i>T</i> chemistry	IR
$\text{HD}, \text{DCO}^+, \text{DCN}, \text{H}_2\text{D}^+$	rotational	photochemistry deuteration	FIR, submm/mm
$\text{CS}, \text{HC}_3\text{N}$	rotational	turbulence	submm/mm

due to energy partitioning into a multitude of levels, and the limitations in sensitivity of the present-day facilities. The situation will change when the Atacama Large Millimeter/Submillimeter Array (ALMA) becomes fully operational by the end of 2013, bringing unprecedented sensitivity and spatial and spectral resolution. This will allow searches for complex species at low spatial resolution (to maximize sensitivity) and detection of strong molecular emission from inner regions of protoplanetary disks at high resolution ($r \gtrsim 10$ – 20 AU). The first discovery of a somewhat heavier molecule with ALMA was the detection of cyclopropenylidene, $\text{c-C}_3\text{H}_2$, in the disk around TW Hya.¹⁴⁷

A general result of these molecular line studies is evidence for the depletion of molecules relative to molecular abundances observed in the interstellar medium^{50,148} (see Figure 5). This is caused primarily by two effects. First, freeze-out (or “depletion”) of molecules onto dust grains occurs in cold disk midplanes, where later some of these ices may become incorporated in icy bodies such as comets. Second, molecules are destroyed by photodissociation in disk atmospheres. Indeed, photodissociation products like CN and the elevated CN/HCN ratios point to the presence of photon-dominated regions at disk surfaces.

3.1.2. Results from Far-Infrared Spectroscopy. The Herschel far-infrared observatory with its spectrometer instruments PACS (with a moderate spectral resolution of 1000–4000) and HIFI (with a high spectral resolution up to 10^6) has provided a flood of interesting molecular data on disk chemistry. Apart from the discovery of cold and warm hydroxyl and water in a number of disks^{149–152} and the recent detection of cold water vapor in the TW Hya disk¹⁵³ (see section 4), the observatory revealed warm CO emission in a large number of disks around more massive, hotter Herbig Ae/Be stars.^{150,154,155} The wavelength range of the PACS instrument covers mid- to high-lying rotational *J* transitions (and CO transitions up to *J* = 31–30 could be discovered), demonstrating the presence of gas with temperatures between 100 and 1000 K.¹⁵⁵

In addition, the oxygen fine structure line at 63 μm , and much less frequently the [OI] line at 145 μm , have been

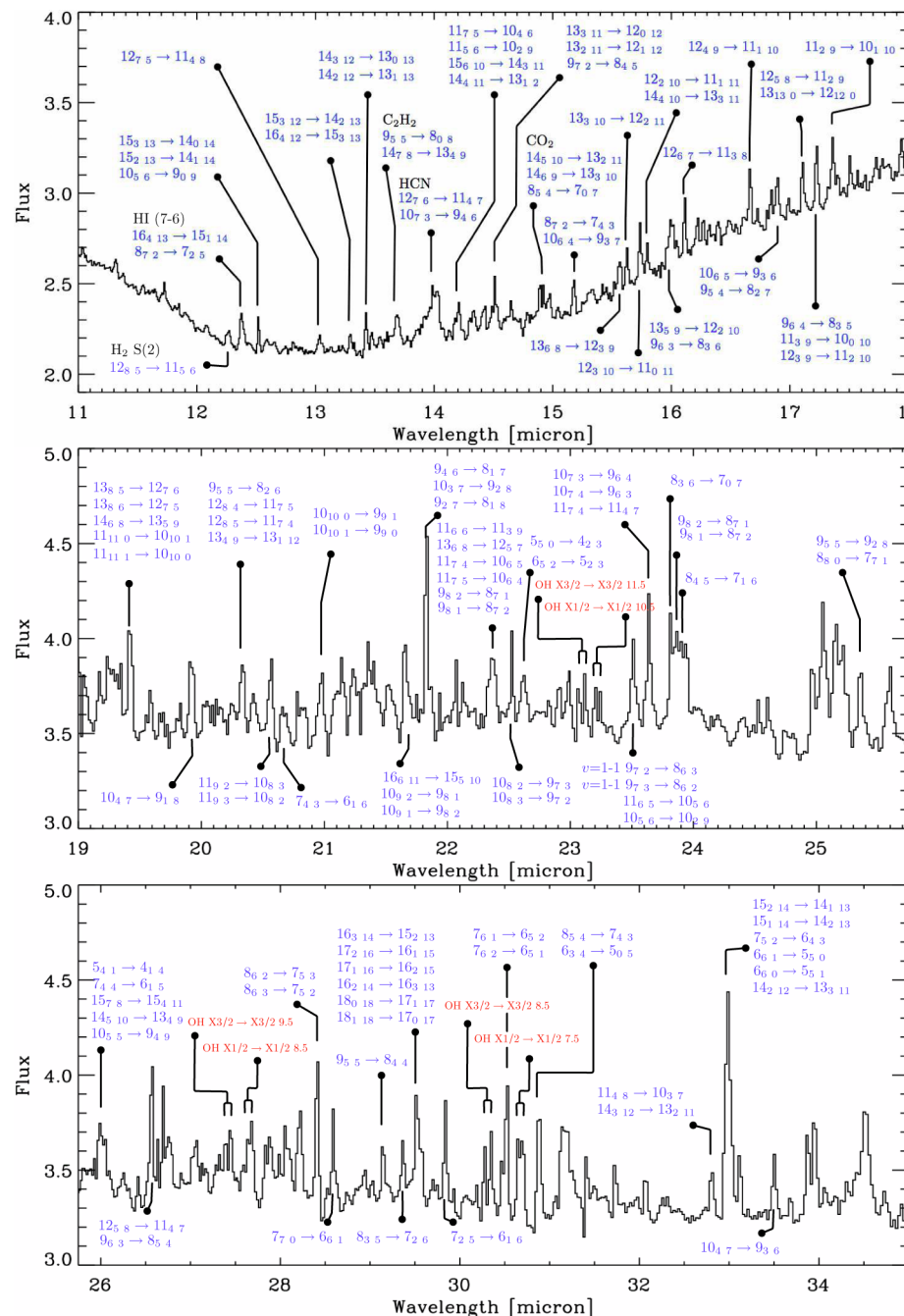


Figure 4. Selected major molecular lines in the Spitzer high-resolution spectrum of a disk around the T Tauri star RNO 90. The transitions refer to the rotational quantum numbers $J_{K_a K_c}$ in the ground vibrational state of water. Rotational transitions with odd sum of K_a and K_c correspond to ortho nuclear spin configurations. Reprinted with permission from ref 167. Copyright 2010 American Astronomical Society.

observed in a number of protoplanetary disks with Herschel.¹⁵⁰ The fine structure line of neutral atomic carbon at $158\ \mu\text{m}$ has also been detected, albeit much less frequently than was anticipated from preliminary modeling.¹⁵⁶ A surprise was the discovery of CH^+ in the disks surrounding the two Herbig Ae stars HD 100546¹⁵⁷ and HD 97048.¹⁵⁰ The main formation pathway for this ion is the endothermic reaction (with an activation energy of $\sim 4500\ \text{K}$) between C^+ and molecular hydrogen, implying that CH^+ is tracing warm gas in the inner disk atmosphere. An alternative explanation is a steady fragmentation of PAHs by intense stellar high-energy radiation, releasing aromatic rings and its “debris”.

3.1.3. Results from Mid- and Near-Infrared Spectroscopy. Despite the relatively low spectral resolution provided by the infrared spectrometer on board the Spitzer observatory (resolution of 90–600 over the wavelength range from 5.3 to $38\ \mu\text{m}$), this mission provided extremely interesting constraints on disk chemistry in the planet-forming zones. Apart from the first discovery of a forest of emission lines from hot H_2O and OH in a number of disks (see Figure 4), CO_2 and organic molecules such as HCN and C_2H_2 could be discovered.^{158–164} On the basis of a comparison between disks around Sun-like stars and cool stars/brown dwarfs, a significant underabundance of HCN relative to C_2H_2 was found in the disk surface of cool

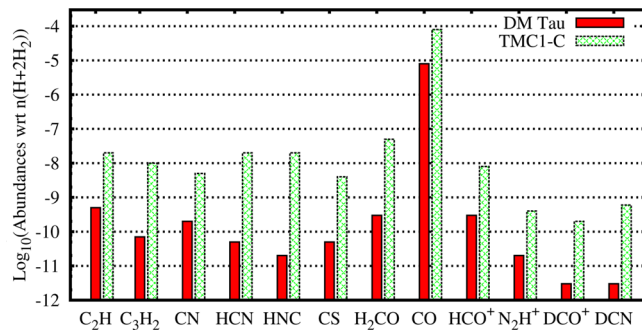


Figure 5. Observed fractional abundances (with regard to the amount of hydrogen nuclei) in the disk around the Sun-like T Tauri star DM Tau and the prestellar core TMC 1-C (Cyanopolyne peak). Data derived from refs 56,68,141,142,144,176–181.

stars.¹⁶⁰ This difference between the two classes of objects indicates different chemical regimes due to large differences in the UV irradiation of their disks. Additionally, strong vibration–rotation absorption bands of CO₂, C₂H₂, and HCN could be discovered in disk systems seen edge-on.^{165,166}

The high temperatures between a few 100 K and a few 1000 K and relatively high densities of $>10^8 \text{ cm}^{-3}$ in the very inner regions of protoplanetary disks are appropriate for excitation of rotational–vibrational molecular transitions. Indeed, rotational–vibrational emission of CO at 4.7 μm has been frequently observed in disks around Herbig Ae stars and T Tauri stars.^{168,169} An analysis of the excitation conditions and velocity profiles suggests that the lines originate from a range of radii from about 0.1 AU out to 1–2 AU.¹⁷⁰ In a number of objects, CO overtone emission at 2.3 μm has been observed and traces hot and very dense gas close to the star.¹⁷¹ In addition, high-resolution near-infrared spectroscopy (with spectral resolution between 25 000 and 96 000) with the

CRIRES instrument at the Very Large Telescope in Chile and the NIRSPEC instrument at the Keck telescope revealed the presence of H₂O, OH, HCN, and C₂H₂ in the very inner disk regions.¹⁶⁴

The presence of the larger PAH molecules in disk surface layers would have important implications for their gas temperature through photoelectric heating and chemistry on their surfaces, including the formation of molecular hydrogen.¹⁷² Infrared emission from PAHs has mostly been observed from the disks around Herbig Ae stars,¹⁷³ with many nondetections toward the T Tauri disks.^{174,175} The overall PAH emission strength is generally higher in targets with a flared disk geometry, pointing to the importance of the radiation field. The relative differences in the IR emission features are mainly caused by chemical differences, especially the ratio of aromatic to aliphatic components induced by the stellar UV radiation field.¹⁷³

3.2. Refractory Grains and Molecular Ices

Ground-based infrared observations in the 8–13 μm atmospheric window and spectroscopic data from the Infrared Space Observatory, the Spitzer satellite, and the Herschel space mission have provided a very rich collection of infrared spectra of protoplanetary disks around young stars. The mid-infrared spectra of T Tauri stars and Herbig Ae/Be stars are dominated by emission features produced by vibrational resonances in amorphous and crystalline silicates, see Figure 6 (see refs 17,182 for reviews). The emission of the silicate dust particles comes from the optically thin warm surface layer of disks with typical temperatures above 100 K. The comparison between calculated absorption cross sections and fluxes based on experimentally determined optical properties and the observed silicate emission features led to the conclusion that a mixture of amorphous silicates with olivine and pyroxene stoichiometry, crystalline forsterite and enstatite, and in some cases silica can

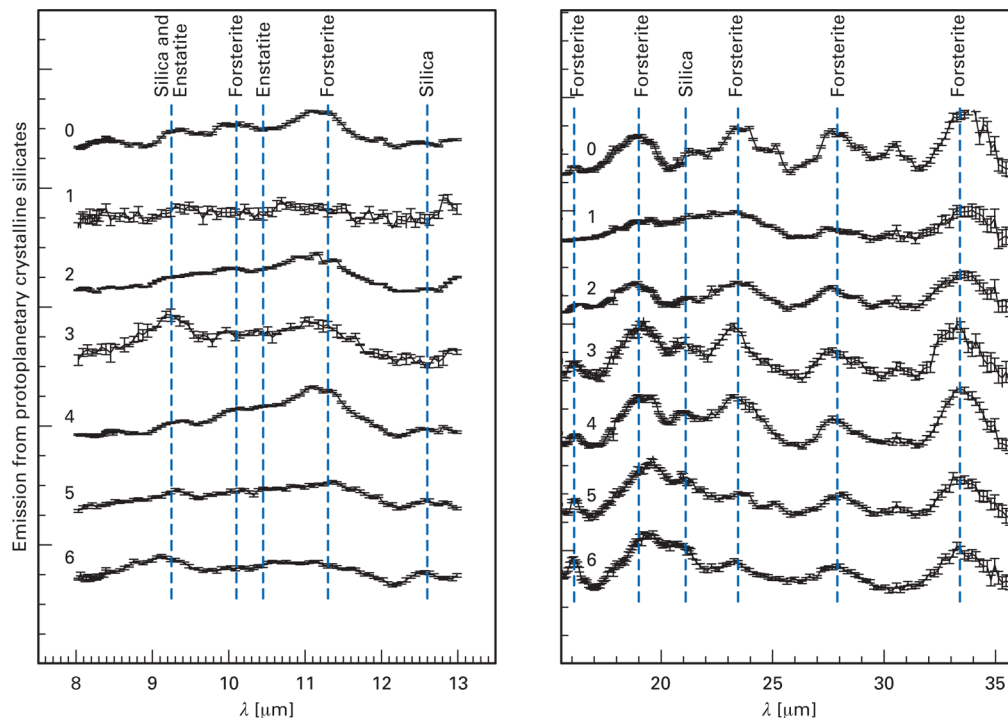


Figure 6. Emission bands of crystalline silicates as observed with Spitzer in the spectra of several T Tauri stars. The amorphous silicate and PAH features are removed from the spectra to enhance the contrast. Data derived from ref 17.

Table 2. Chemical Reactions Active in Disks

process	example	midplane $r > 20$ AU	molecular layer $r > 20$ AU	atmosphere $r > 20$ AU	inner zone $r < 20$ AU
Bond Formation					
radiative association	$\text{C}^+ + \text{H}_2 \rightarrow \text{CH}_2^+ + h\nu$	X	X	X	X
surface formation	$\text{H} + \text{H} \text{gr} \rightarrow \text{H}_2 + \text{gr}$	X	X	0	0
three-body	$\text{H} + \text{H} + \text{H} \rightarrow \text{H}_2 + \text{H}$	0	0	0	X
Bond Destruction					
photodissociation	$\text{CO} + h\nu \rightarrow \text{C} + \text{O}$	0	X	X	X
dissociation by CRP	$\text{H}_2 + \text{CRP} \rightarrow \text{H} + \text{H}$	X	X	0	0
dissociation by X-rays		0	X	X	X
dissociative recombination	$\text{H}_3\text{O}^+ + \text{e}^- \rightarrow \text{H}_2\text{O} + \text{H}$	X	X	X	X
Bond Restructuring					
neutral-neutral	$\text{O} + \text{CH}_3 \rightarrow \text{H}_2\text{CO} + \text{H}$	X	X	0	X
ion-molecule	$\text{H}_3^+ + \text{CO} \rightarrow \text{HCO}^+ + \text{H}_2$	X	X	X	X
charge transfer	$\text{He}^+ + \text{H}_2\text{O} \rightarrow \text{He} + \text{H}_2\text{O}^+$	X	X	X	X
Unchanged Bond					
photoionization	$\text{C} + h\nu \rightarrow \text{C}^+ + \text{e}^-$	0	X	X	X
ionization by CRP	$\text{C} + \text{CRP} \rightarrow \text{C}^+ + \text{e}^-$	X	X	0	0
ionization by X-rays		0	X	X	X

best explain the observed spectra.¹⁸³ A comprehensive study of high-quality Spitzer spectra of Herbig Ae/Be stars indicates that porous iron-poor amorphous silicates are responsible for the observed 10 μm features produced by the Si–O stretching mode. In addition, the analysis of the strength and shape of the 10 μm silicate feature has provided strong evidence for considerable grain growth to micrometer-sized particles, which are much larger than the “pristine” sub-micrometer-sized dust grains of the interstellar medium (see refs 17,182 for a review). The solid-state infrared bands become flatter and finally disappear when the sizes of the emitting grains become comparable to the wavelength, i.e., for the 10 μm silicate feature this occurs for grains bigger than several micrometers.^{17,183,184} The observed anticorrelation between the size of the amorphous grains and disk flaring points to the combined effect of coagulation and sedimentation.^{183,185,186} Coagulation leads to depletion of growing dust grains from the extended disk atmosphere, as they are gravitationally settling toward the midplane. Consequently, the surface where disks become optically thick moves along, and the disk vertical structure becomes flatter. Evidence for much larger grains up to centimeter sizes comes from the analysis of dust emission at millimeter and even centimeter wavelengths.^{187–190}

Sharp bands of crystalline silicates can be observed in nearly all disk spectra (see Figure 6). The fractional abundances of crystalline silicates cover values between $\approx 1\%$ and 30%. The observed bands are best explained by emission from forsterite and enstatite particles. The forsterite-to-enstatite mass ratio changes with location, with lower values in the inner disks and higher values in the outer disks. The analysis of the 69 μm feature produced by forsterite particles clearly shows that the particles are nearly iron-free.^{154,191} The presence of crystalline silicates in protoplanetary disks is a finding that is in strong contrast to the properties of dust in molecular clouds and the diffuse interstellar medium, where crystalline silicates are not found. The presence of crystalline silicates in disks can only be explained by strong thermal processing in protoplanetary disks either through thermal annealing and condensation in the inner regions of disks¹⁹² or shock heating at several astronomical units from the central star.¹⁹³ None of these theories is without problems and fully consistent with the observational constraints. An interesting piece of information to address the

puzzle of crystal formation in disks was the observation of *in situ* crystal formation through the annealing of dust in the surface layers of the protoplanetary disk around the eruptive star EX Lupi.^{194,195}

Protoplanetary disks should certainly contain other solid phases such as Fe and FeS grains as well as carbonaceous particles.^{196,197} However, such particles have not been discovered by infrared spectroscopy so far either because they do not show intrinsic infrared bands, they are too large in size to show strong features, or they are simply not abundant enough. In a few disks around Herbig Ae/Be stars infrared features at 3.43 and 3.53 μm have been detected.¹⁹⁸ These features were identified as the vibrational modes of hydrogen-terminated facets of nanodiamonds.¹⁹⁹

In the rare situation of disks seen edge-on, evidence for the presence of molecular ices can be found through their absorption features.^{200,201} An interesting example of such an object is the source CRBR 2422.8–3423,^{202,203} where at least part of the H_2O and CO_2 absorption features are apparently produced in the disk. In addition, a feature at 6.85 μm , tentatively attributed to NH_4^+ , shows evidence for grain heating to ≈ 50 K and is certainly produced in the disk around this object.

Librational features of crystalline water ice at 44 and 63 μm have the potential to provide important information about the frozen water reservoir. So far, these features have only been detected in very few objects,²⁰⁴ but the Herschel mission should find the 63 μm feature in some additional disk sources.²⁰⁵

3.3. Main Chemical Processes

As discussed in section 2 protoplanetary disks are characterized by strong vertical and radial temperature and density gradients together with vastly different radiation fields at various disk locations. These locally different disk properties imply a rich and diverse disk chemistry, including photochemistry, molecular-ion reactions, neutral–neutral reactions, gas–grain surface interactions, and grain surface reactions. A summary of relevant reactions is provided in Table 2.

On the basis of the radially decreasing temperature, disk chemistry can be roughly divided between inner disk chemistry ($\lesssim 20$ AU) and chemistry in the outer disk regions beyond 20 AU. Observationally the products of inner disk chemistry are

best characterized by infrared spectroscopy, whereas the outer disk is the domain of (sub)millimeter observations.

Inner disks are characterized by their high temperatures (from about 100 to 5000 K) and high densities up to 10^{12} cm^{-3} (and more). At these high temperatures and densities in the disk, chemistry approaches a quasiequilibrium. In the absence of intense sources of ionizing radiation, neutral–neutral reactions with barriers ($\gtrsim 100\text{--}1000 \text{ K}$ or $\gtrsim 0.2 \text{ eV}$) start playing an important role in the densest warm disk inner regions.²⁰⁶ Thus, the inner disk chemistry comes closer to conditions known for “terrestrial” chemistry, driven by 3-body collisions, although characteristic time scales of the disk chemical processes are usually much longer.⁶⁸ At the very high densities, $> 10^{12} \text{ cm}^{-3}$,²⁰⁷ 3-body reactions become important in inner disks, such as the formation of molecular hydrogen by collisions of two hydrogen atoms and another particle that takes away the excess of energy of formation.

At the high temperatures and densities of inner disks, molecules should be abundant in the gas phase until they are destroyed by thermal dissociation ($T \gtrsim 2500\text{--}3500 \text{ K}$). Chemical models of the inner disk chemistry^{61,208–212} predict high abundances of H₂O and CO vapor at 1 AU and the presence of N-bearing molecules (NH₃, HCN, HNC) and a variety of hydrocarbons (e.g., CH₄ and C₂H₂). Radiation fields for higher-mass stars may lead to the destruction of water and the formation of OH molecules in inner disk atmospheres.²¹³

In contrast to “terrestrial” chemistry typical for very inner dense disk regions, high-energy radiation and cosmic rays are key drivers of outer disk chemistry.^{32,42,44,49,71,96,98,214–216} The ionizing radiation leads to the production of various ions, including H₃⁺. The proton transfer processes from ions to other neutrals drive rapid ion–molecule chemistry.^{217–220} The ion–molecule processes are mostly barrierless and thus effective even at temperatures well below 100 K, particularly in reactions involving long-range Coulomb attraction between an ion and a polarizable molecule.

Another important feature of disk chemistry is the freeze-out of molecules at low temperatures in the outer disks. These molecules are then no longer available for gas-phase chemistry. The ices on dust surfaces may remain chemically active. These ices no longer exist at the high temperatures of the inner disks due to sublimation, where dust grains are bare solids. The sublimation of water ice occurs at about 150 K and defines the so-called “water snow line”, which is located at 2–3 AU in the early solar nebula.^{221–224} The CO “snow line” is located at a larger radial distance of about 20 AU (beyond the orbit of Uranus), where the gas temperature drops below 20 K. We should note that the positions of the “snow lines” evolve with evolutionary stage of the disks and are a function of the luminosity of the central star.^{51,225}

In the outer disk ($r \gtrsim 20 \text{ AU}$) we can distinguish three chemically different regimes depending on the vertical disk location.²¹⁴ In the disk surface layers stellar UV radiation and the interstellar radiation field ionize and dissociate molecules and drive ion–molecule chemistry. In this photon-dominated region photochemistry is particularly important and depends strongly on the strength and shape of the radiation field. T Tauri stars emit intense nonthermal UV radiation from the accretion shock, often in a pronounced Lyman α line,^{226,227} while the hotter Herbig Ae/Be stars produce large amounts of thermal UV emission. The integrated flux of the stellar UV radiation at 100 AU can be higher by a factor of 100–1000 for a T Tauri disk⁸⁷ and 10^5 for a Herbig Ae disk,^{99,228} respectively,

compared to the interstellar radiation field.²²⁹ Photodissociation operates very differently for different molecules and is a sensitive function of the actual radiation field. As an example, Lyman α photons will selectively dissociate HCN and H₂O, while other molecules such as CO and H₂ are practically unaffected.⁴⁴ Many of the other important molecules such as CO and H₂ are dissociated by FUV radiation at wavelengths between 91.2 and 110 nm.^{44,230} Since the dissociative destruction of the abundant H₂ and CO molecules operates through photoabsorption at discrete wavelengths, isotopically selective photodissociation based on various degrees of self-shielding is possible.^{46,231} Selective photodissociation of CO by the interstellar radiation field can also play an important role at the far outer edges of disks as has been demonstrated for the DM Tau disk.¹³⁷

The keV X-ray radiation is another important energy source for disk chemistry. Unlike the stellar UV luminosities, the stellar X-ray luminosities decline from T Tauri to Herbig Ae/Be stars. The representative median values for T Tauri stars are $\log(L_X/L_{\text{bol}}) \approx -3.5$ (where L_{bol} is the total bolometric luminosity of the stars), which gives $L_X \approx 3 \times 10^{29} \text{ erg s}^{-1}$ (with an uncertainty of an order of magnitude).^{88,232} This radiation is generated by coronal activity similar to our Sun but $\gtrsim 1000$ times stronger, which is driven by magnetic fields generated by an dynamo mechanism in convective stellar interiors. In contrast, Herbig Ae stars have weak surface magnetic fields due to their nonconvective interiors, and consequently, their X-ray luminosities are $\gtrsim 10$ times lower than those of T Tauri stars.⁹⁰ The X-ray emitting source is often posited to be located high above the stellar photosphere, at distances of several stellar radii, and thus, X-ray photons reach the disk atmosphere at an oblique angle and are able to penetrate deeper into the disk compared to the stellar FUV photons.⁵² Also, having average energies of several keV, the X-ray photons are able to penetrate through higher gas columns of $\sim 0.1\text{--}1 \text{ g cm}^{-2}$ compared to the FUV photons ($< 0.01 \text{ g cm}^{-2}$). The unique role of X-rays in disk chemistry is their ability to ionize He (with a huge ionization potential of 24.6 eV), producing chemically active He⁺. Due to its high electron affinity, ionized helium is able to destroy the tightly bound CO molecules (and other gas species), replenishing elemental carbon and oxygen back to the gas. This process drives a rapid and rich gas-phase hydrocarbon chemistry and enriches overall gas molecular complexity.

Adjacent to the disk surface is a warm molecular layer ($T \approx 30\text{--}70 \text{ K}$), where the CO molecule is protected from freeze-out. This region is partly shielded from stellar and interstellar UV/X-ray radiation allowing a rich molecular chemistry. Water is still frozen onto dust grains, removing most of the oxygen from the gas phase. This implies relatively high gas C/O ratios close or even larger than 1, leading to a carbon-based chemistry. Finally, UV photons may drive photodesorption in less opaque regions with experimentally determined rates available for CO, H₂O, CH₄, and NH₃.^{233–236}

The third layer is located deep in the interior of the disk close to the midplane. This layer is completely shielded from high-energy radiation (apart from cosmic ray particles and locally produced energetic particles due to decay of short-lived radionuclides). The temperature drops below 20 K; freeze-out of molecules and hydrogenation reactions on grain surfaces dominate the chemistry. The freeze-out time scale t_{freeze} for the standard gas-to-dust mass ratio of 100 and a sticking probability of 1 can be roughly estimated by the following expression:

Table 3. Chemical Models of Protoplanetary Disks

year	ref	disk structure	viscosity	UV	X-rays	CRP	gas thermal balance		dust grain sizes	reactions	gas-grain	time-dep	chemistry dynamics
							high-energy radiation	rad advection					
1996	Aikawa et al. ^{258,259}	MMSN, ²⁸⁸ steady	passive	no	no	10^{-17} s^{-1}	no	no	$0.1 \mu\text{m}$	gas-grain	yes	no	rad advection
≥ 1998	Aikawa et al. ^{207,269,289}	$1 + 1\text{D},^{69}$ steady	$\alpha = 0.01$	no	no	10^{-17} s^{-1}	no	no	$0.1 \mu\text{m}$	gas-grain	yes	no	rad advection
1998	Willacy et al. ²⁰⁸	$1 + 1\text{D}$, steady MMSN, ²⁸⁸ steady	$\alpha = 0.01$ passive	no	$1 + 1\text{D}$	10^{-17} s^{-1}	no	uniform	$0.1 \mu\text{m}$	gas-grain	yes	no	gas-grain
≥ 1999	Aikawa and Herbst ^{214,270}	$1 + 1\text{D},^{290}$ steady	passive	$1 + 1\text{D}$	no	10^{-17} s^{-1}	no	uniform	gas-grain	yes	no	gas-grain	gas-grain
2000	Willacy and Langer ⁴¹	$(1+1)\text{D},^{292}$ steady	passive	$1 + 1\text{D}$	no	10^{-17} s^{-1}	no	uniform	gas-grain	yes	no	gas-grain	gas-phase
2001	Kamp and van Zadelhoff ²⁹¹	$1 + 1\text{D},^{92,263}$ steady	$\alpha = 0.01$	$1 + 1\text{D}$	no	10^{-17} s^{-1}	no	power law	$0.1 \mu\text{m}$	gas-grain	no	gas-phase	gas-phase
2002	Aikawa et al. ²¹⁵	$1 + 1\text{D},^{92,263}$ steady	$\alpha = 0.01$	$1 + 1\text{D}$	no	10^{-17} s^{-1}	no	power law	$0.1 \mu\text{m}$	gas-grain	yes	no	gas-grain
2002	Markwick et al. ^{209,293}	$1 + 1\text{D}$, steady $1 + 1\text{D},^{92,263}$ steady	$\alpha = 0.01$ $\alpha = 0.01$	$1 + 1\text{D}$	3-layer no	10^{-17} s^{-1}	no	uniform	$0.1 \mu\text{m}$	gas-grain	yes	no	gas-grain
2003	van Zadelhoff et al. ⁴²	$1 + 1\text{D},^{92,263}$ steady	$\alpha = 0.01$	2D	no	10^{-17} s^{-1}	no	uniform	$0.1 \mu\text{m}$	gas-grain	yes	no	gas-phase
2004	Glassgold et al. ^{100,294}	$1 + 1\text{D},^{92}$ steady	$\alpha = 0.01$ –, 2.0	no	$1 + 1\text{D}^{52}$	no	yes	power law	gas-phase	yes	no	gas-phase	gas-phase
≥ 2004	Gorti and Hollenbach ^{96,97}	$1 + 1\text{D}$, steady	passive	$1 + 1\text{D}$	$1 + 1\text{D}$	$1 + 1\text{D}$	yes	power law	gas-phase	yes	no	gas-phase	gas-phase
2004	Lignor et al. ⁶¹	$1 + 1\text{D}$, steady	$\alpha = 0.005$, 0.01	$1 + 1\text{D}$	3-layer ²⁰⁹	1D	no	uniform	gas-grain	yes	no	rad advection	vert mixing
2004	Jonkheid et al. ^{99,297}	$1 + 1\text{D},^{92}$ steady	$\alpha = 0.01$	$1 + 1\text{D}$	no	$5 \times 10^{-17} \text{ s}^{-1}$	yes	power law, evol $m_{\text{dust}}/m_{\text{gas}}$	gas-phase	yes	no	gas-phase	gas-phase
2004	Kamp and Dullemond ⁹⁵	$1 + 1\text{D},^{298}$ steady	passive	$1 + 1\text{D}$	no	yes	yes	0.1 μm	gas-phase	no	no	gas-phase	gas-phase
2004	Semenov et al. ⁴³	$1 + 1\text{D},^{92}$ steady	$\alpha = 0.01$	$1 + 1\text{D}$	$1 + 1\text{D}^{52}$	1D	no	0.1 μm	gas-grain	yes	no	gas-phase	gas-phase
2005	Ceccarelli and Dominik ^{271,299}	$2\text{D},^{300}$ steady	passive	no	no	3×10^{-19} to $3 \times 10^{-15} \text{ s}^{-1}$	no	0.1 μm	gas-phase, D	no	no	gas-phase, gas-grain	gas-grain
≥ 2005	Nomura et al. ^{266,301}	$1 + 1\text{D}$, steady	$\alpha = 0.01$	$1 + 1\text{D}$	$1 + 1\text{D}$	1D	yes	power law ²⁶⁴	gas-grain	yes	no	gas-phase	gas-phase
2006	Aikawa and Nomura ²⁶⁰	$1 + 1\text{D},^{301}$ steady	$\alpha = 0.01$	$1 + 1\text{D}$	no	10^{-17} s^{-1}	yes	power law, 10 μm to 10 cm	gas-grain	yes	no	gas-phase	gas-phase
≥ 2006	Ilgner and Nelson ⁵³	$1 + 1\text{D}$, steady	$\alpha = 0.01$	$1 + 1\text{D}$	$1 + 1\text{D}$	no	no	uniform	gas-phase, gas-grain	yes	no	gas-phase	gas-phase
2006	Semenov et al. ²⁷⁸	$1 + 1\text{D},^{92}$ steady	$\alpha = 0.01$	$1 + 1\text{D}$	$1 + 1\text{D}^{52}$	1D	no	0.1 μm	gas-grain	yes	2D mixing	gas-grain	gas-grain
2006	Willacy et al. ⁶²	$1 + 1\text{D}$, steady	$\alpha = 0.01$	$1 + 1\text{D}$	no	10^{-17} s^{-1}	no	power law	gas-grain	yes	vert mixing	gas-grain	gas-grain
2007	Aikawa ⁶³	$1 + 1\text{D},^{301}$ steady	$\alpha = 0.01$	$1 + 1\text{D}$	no	10^{-17} s^{-1}	no	MRN ³⁰² law, $r_{\text{max}} = 10 \mu\text{m}$	gas-grain	yes	vert mixing	gas-grain	gas-grain
≥ 2007	Dutrey et al. ^{37,141,303}	$1 + 1\text{D}$, steady	$\alpha = 0.01$ –0.03	$1 + 1\text{D}$	$2\text{D}^{52,267}$	1D	no	0.1 μm	gas-grain	yes	no	gas-phase	gas-phase
2007	Jonkheid et al. ³⁰⁴	$2\text{D},^{300}$ steady	passive	2D	no	$5 \times 10^{-17} \text{ s}^{-1}$	yes	power law, evol $m_{\text{dust}}/m_{\text{gas}}$	gas-phase, gas-grain	yes	no	gas-phase	gas-phase
2007	Turner et al. ^{64,279}	3D MHD, shear-box	3D MHD	no	no	1D	no	0.1 μm	gas-phase, reduced ¹⁰⁵	yes	3D mixing	gas-phase	gas-phase

Table 3. continued

year	ref	high-energy radiation						chemistry		
		disk structure	viscosity	UV	X-rays	CRP	gas thermal balance	dust grain sizes	reactions	time-dep
2007	Willacy ²⁷²	1 + 1D, ³⁰⁶ steady	$\alpha = 0.01$	1 + 1D	no	10^{-17} s^{-1}	no	power law	gas-grain, D	yes
≥ 2007	Willacy and Woods ^{210,273,274}	1 + 1D, ³⁰⁶ steady	$\alpha = 0.01, 0.025$	2D ⁴⁰	1 + 1D ⁹⁶	1D	yes	power law	gas-grain, D	yes
2008	Agrindel et al. ²⁶¹	1 + 1D, ^{92,263} steady	$\alpha = 0.01$	1 + 1D	no	10^{-17} s^{-1}	no	MRN ³⁰² law	gas-phase	yes
2008	Chapillon et al. ^{307,308}	(1+) 1D, steady	passive	1 + 1D	no	10^{-17} s^{-1}	no	power law evol. $m_{\text{dust}}/m_{\text{gas}}$	gas-phase	yes
2008	Vasyunin et al. ³⁰⁹	1 + 1D, ⁹² steady	$\alpha = 0.01$	1 + 1D	1 + 1D ⁵²	10^{-17} s^{-1}	no	0.1 μm	gas-grain	yes
2009	Gorti et al. ⁴⁵	1 + 1D, ⁶⁹ evolv.	$\alpha = 0.01, 0.001, 0.1$	1 + 1D	1 + 1D	1D	yes	0.3 μm	gas-phase	yes
2009	Hersant et al. ⁶⁶	2-layer	passive	1 + 1D	no	1D	no	0.1 μm	gas-grain	yes
2009	Nomura et al. ²⁷⁵	1 + 1D, steady	$\alpha = 0.01$	1 + 1D	1 + 1D ²⁶⁶	1D	yes	power law ²⁶⁴	gas-grain	yes
≥ 2009	Visser et al. ^{310,276}	2D, evol	$\alpha = 0.01$	1 + 1D	no	$5 \times 10^{-17} \text{ s}^{-1}$	no	0.1 μm	gas-grain	yes
≥ 2009	Woithee et al. ^{157,265,268,285,311,312}	2D, ³¹³ steady	α	2D	2D	1D	yes	power law	gas-grain	no
2010	Henning et al. ⁴⁷	1 + 1D, steady	$\alpha = 0.01-0.03$	1 + 1D	2D ⁵²	1D	no	0.1 μm	gas-grain	yes
≥ 2010	Wash et al. ^{49,262}	1 + 1D, steady	$\alpha = 0.01$	1 + 1D	1 + 1D ²⁶⁶	1D	yes	power law ²⁶⁴	gas-grain	yes
2011	Cleevies et al. ³¹⁴	1 + 1D, steady	passive	2D, ⁹¹ Ly α	1 + 1D ⁵²	10^{-17} s^{-1}	no	power law ²⁶⁴	gas-grain	yes
≥ 2011	Dutrey et al. ¹⁴²⁻¹⁴⁵	2-layer ⁶⁶	passive	1 + 1D	no	1D	no	0.1 μm	gas-grain	yes
2011	Fogel et al. ²¹⁶	1 + 1D, steady	$\alpha = 0.01$	2D, ⁹¹ Ly α	1 + 1D ⁵²	1D	no	power law, settling	gas-grain	yes
2011	Ilee et al. ²⁸²	3D HD	grav instab	no	no	1D	no	0.1 μm	gas-grain	yes
2011	Heinzeller et al. ⁶⁷	1 + 1D, steady	$\alpha = 0.01$	1 + 1D	1 + 1D ²⁶⁶	1D	yes	power law ²⁶⁴	gas-grain	yes
2011	Najita et al. ²¹²	1 + 1D, ⁹² steady	$\alpha = 0.01$	no	1 + 1D ⁵²	no	yes	power law	gas-phase	no
2011	Semenov and Wiebe ⁶⁸	1 + 1D, steady	$\alpha = 0.01$	1 + 1D	2D ¹⁰⁰	1D	no	0.1 μm	gas-grain	yes
2011	Vasyunin et al. ⁹⁸	1 + 1D, steady	$\alpha = 0.01$	1 + 1D	1 + 1D ⁵²	1D	no	2D evol ^{102,105}	gas-grain	yes
2012	Bruderer et al. ¹⁵⁶	2D, ³¹⁵ steady	passive	2D	1 + 1D ³¹⁶	1D	yes	MRN ³⁰² law	gas-grain	no
2013	Akimkin et al. ⁷¹	1 + 1D, steady	$\alpha = 0.01$	1 + 1D	2D ²⁶⁷	1D	yes	2D evol ^{105,317}	gas-grain	yes

$$t_{\text{freeze}} \approx \frac{10^9 \text{ cm}^{-3}}{n_{\text{H}}} \frac{a_d}{0.1 \mu\text{m}} \text{ years} \quad (2)$$

Here, n_{H} is the gas particle density (in cm^{-3}) and a_d is the typical grain radius (in μm). The freeze-out time scales in the cold midplanes of protoplanetary disks (with typical densities of $\sim 10^6$ – 10^8 cm^{-3}) are on the order of 10– 10^3 years, indicating that most of the material in the gas phase is frozen-out within a fraction of the disk lifetime. The most important desorption process for volatiles such as CO, N₂, and CH₄ is thermal desorption. In addition, cosmic ray and X-ray spot heating may release mantle material back to the gas phase.^{237–239}

3.4. Status of Chemical Models for Protoplanetary Disks

In this section we provide an overview of the status of chemical models of protoplanetary disks, but do not discuss in detail chemical models tuned to the specific conditions of the solar nebula.

Historically, the first chemical models were developed for studies of the chemical composition of planets and primitive bodies in the solar system.²⁴⁰ These models were usually restricted to the inner, planet-forming midplane region of the nebula ($r \lesssim 10$ – 30 AU). In these models “dark” conditions were assumed, with cosmic rays and the decay of short-living radionuclides as the only ionizing sources. These warm, dense, and dark conditions imply that chemical equilibrium is likely to be reached within several million years of the nebula’s lifetime. Consequently, thermodynamical equilibrium was usually assumed in the chemical models of the early inner solar nebula. The primary focus of research of these nebular models was sublimation and condensation of various types of minerals as a function of distance, and the impact of nebular dynamics and evolution on these processes.^{241–244} We should note however that even for the chemical models of the inner solar nebula the assumption of chemical equilibrium may not be appropriate because radiation is certainly more important than previously assumed.

For example, comprehensive studies of dust evolutionary processes and the interaction of high-energy radiation with gas and dust, together with radial advective transport, were performed by the Heidelberg ITA group.^{58,59,192,245–251} Initially in these studies ice mantle evaporation and accumulation, and dust evaporation and destruction, were included in the models. Then, ionization of nebular matter by cosmic rays, radionuclides, and UV photons was investigated. Later, various annealing and combustion processes for carbonaceous dust and metamorphosis of silicate dust were considered. Similar studies that investigated the evolution of more volatile materials, in particular, water ice, and isotopic fractionation, were conducted.^{60,121,252–254} In ref 65 a self-consistent chemodynamical model of the solar nebula was presented, which coupled 2D-hydrodynamics with extended gas-phase neutral–neutral chemistry and the consideration of dynamical transport processes. A series of studies were devoted to explain the origin of complex organic materials found in carbonaceous meteorites, which show extreme hydrogen and nitrogen isotopic anomalies (see section 6). The importance of nonequilibrium chemistry in the outer, more distant, or more UV-irradiated parts of the solar nebula was also recognized, albeit not widely considered.^{255–257}

In contrast to the chemical models of the solar nebula, chemical models of protoplanetary disks are mostly based on detailed chemical kinetics models, including a multitude of

processes with hundreds and thousands of chemical reactions (see Table 3). This makes extensive disk chemical modeling a computationally intensive task, and thus, many modern astrochemical models are decoupled from disk dynamics.^{41,42,95,156,208,209,215,228,258–262} The underlying disk physical structure is often based on a steady-state, 1 + 1D α -model in vertical hydrostatic equilibrium,^{92,141,263} mostly with uniformly distributed, single-sized dust grains or power law size distributions with various minimum and maximum cutoff grain sizes.²⁶⁴ While in the past equilibrium between dust and gas temperatures throughout the disk was typically assumed, this simplistic assumption tends to be relaxed in recent models, where chemistry in disk atmospheres and gas thermal balance are calculated.^{71,95,265} This, however, requires detailed calculation of gas thermal balance, including various heating and cooling processes such as photoelectric heating of gas by FUV-irradiated dust and PAHs, gas–grain collisions, dust heating and cooling, fine-structure line cooling via atomic species, etc., which is a nontrivial undertaking.

In contrast to the solar nebula models, most of the disk chemical models include photoprocessing and a detailed treatment of the far-UV radiative transfer, either in an 1 + 1D plane-parallel²⁶⁶ or a full 2D approximation,⁴² also including resonant scattering of Ly α photons.⁹¹ Almost every disk model includes ionization by cosmic ray particles and many include ionization due to decay of short-living radionuclides. Disk models targeted to investigate chemistry in irradiated disk atmospheres and the molecular layer also include X-ray radiative transport.^{47,52,267,268} In several studies deuterium chemistry was added to the chemical models.^{269–273}

A recent advancement in studies of disk chemistry is the treatment of grain evolution. Grain coagulation, fragmentation, sedimentation, turbulent stirring, and radial transport are all important processes to be taken into account. Grain growth depletes the upper disk layers of small grains and hence reduces the opacity of disk matter, allowing the far-UV radiation to penetrate more efficiently into the disk, and to heat and dissociate molecules deeper in the disk. Also, larger grains populating the disk midplane may delay the depletion of gaseous species because of the reduced total surface area.^{71,98,216,260}

In addition to laminar disk models, a number of chemodynamical models of protoplanetary disks were developed. For instance, chemical evolution in protoplanetary disks with 1D radial advective mass transport was studied.^{207,210,273–275} The transformation of a parental molecular cloud into a protoplanetary disk was studied using a 2D hydrodynamical code with 2D advection flow coupled to gas–grain chemistry.^{46,276} Another class of chemodynamical disk models is based on turbulent diffusive mixing, which smears out chemical gradients, and is modeled in 1D, 2D, or even full 3D^{53–55,62–64,66,68,277–279} (see also section 3.5). In several disk models both advective transport and turbulent mixing were considered,^{61,67} while ref 45 studied photoevaporation of disks and loss of the gas due to the stellar far-UV and X-ray radiation.

All those disk models are mainly axisymmetric models where mass is transported locally. Such models may be inappropriate during the early phases of disk evolution when disks are massive enough to trigger gravitational instabilities.²⁸⁰ Gravitational instabilities produce transient nonaxisymmetric structures in the form of spiral waves, density clumps, etc.,^{31,281} which might explain asymmetries observed in some protoplanetary disks.¹⁸ More importantly, gravitational instabilities lead to efficient

mass transport and angular momentum redistribution, which could be characterized by a relatively high viscosity parameter $\alpha \sim 1$. A first study where these effects were considered along with time-dependent chemistry was recently performed.²⁸²

In the coming years, we can expect that sophisticated multidimensional magneto-hydrodynamical models will be coupled with time-dependent chemistry. First steps in this direction have been made,⁶⁴ where a simple chemical model has been coupled to a local 3D MHD simulation. Another research direction is to add line radiation transfer to the disk chemical models in order to make predictions of line intensities and spectra.^{283–285} In addition, a detailed 2D/3D treatment of the X-ray and UV radiation transfer with scattering is an essential ingredient for realistic disk chemical models.^{42,286} An accurately calculated UV spectrum including Ly α scattering is required to calculate photodissociation and photoionization rates, and shielding factors for CO, H₂, and H₂O.^{91,101,211} In heavily irradiated disk atmospheres many species will exist in excited (ro-)vibrational states, which may then react differently with other species and require addition of state-to-state processes in the models.²⁸⁷ In the outer, cold disk regions addition of nuclear-spin-dependent chemical reactions involving ortho- and para-states of key species is required. Last but not least, a better understanding of surface processes, including nonthermal desorption, chemisorption, high-energy processing of ices, diffusion through the ice mantle, and related factors have to be considered.

3.5. Chemistry and Dynamics

An isotopic analysis of refractory condensates in the most primitive, unaltered chondrites (a class of stony meteorites) shows strong evidence that the elemental composition of the inner part of the solar nebula within about 0.1 to several AU was homogenized during several million years, but not completely.^{80,254} A plausible scenario for such mixing is dynamical transport due to turbulent diffusion and angular momentum removal, combined with a repeated sequence of evaporation and recondensation of solids in the very inner hot nebular region. One of the most notable exceptions is oxygen, which shows anomalous isotopic signatures between all its 3 isotopes at the bulk percent level.^{252,318} The most likely candidates for the production of the oxygen isotopic anomalies are chemical mass-independent fractionation and photochemical self-shielding effects, combined with transport processes. Also, only a small fraction of presolar grains survived the dynamically violent and thermally hazardous process of the solar nebula formation and are routinely found in primitive meteorites.³¹⁹ Thus, the thermally reprocessed solids in the inner solar nebula do not retain much memory of the pristine interstellar chemical composition.^{320,321} In contrast, pristine ices were likely able to survive the formation of the solar nebula in its outer cold regions^{310,322} and later were incorporated into comets.

Another indication that dynamics of the solar nebula was important for its chemical evolution is the rich variety of organic compounds found in carbonaceous meteorites, including amino acids. It has been suggested that complex organics formed just prior or during the formation of planets in heavily irradiated, warm regions of the nebula.^{322–325} Combustion and pyrolysis of hydrocarbons and PAHs at high (~ 1000 K) temperatures and high densities followed by radial outward transport have been proposed as a mechanism by which kerogen-like (mainly aromatic) carbonaceous materials

found in meteoritic and cometary samples were synthesized.³²⁶ A route to a second-generation production of complex organics may be aqueous alteration inside the parent bodies of carbonaceous meteorites, although its role is debated.^{322,324}

The presence of crystalline silicates annealed at temperatures above 800 K in cometary samples collected by the Stardust mission³²⁷ may be further evidence for efficient, large-scale transport of solids in the solar nebula. Evidence for the presence of crystalline silicates in comets has also been found in their infrared spectra.^{328,329} Various transport processes have been suggested, e.g., turbulent mixing, accretion flows, stellar/disk winds, radiation pressure, or aerodynamic sorting (or a combination of all).^{330–333} Alternative mechanisms of the *in situ* production of the crystalline silicates by heating events include frequent electric discharges in a weakly ionized plasma,³³⁴ outbursts of a central star,¹⁹⁴ or shocks.¹⁹³ The omnipresence of high-temperature crystalline silicates observed in other protoplanetary disks and radial variations of the crystallinity fraction advocate for robustness of this crystallization process.^{17,183,184,335,336}

The turbulent nature of protoplanetary accretion disks, as discussed in section 2.1, leads to nonthermal gas motions and radial transport of gas. As turbulence is a 3D-phenomenon driven by a magneto-rotational instability in a rotating gaseous disk, it requires computationally intensive modeling that has only recently become manageable (assuming a simplified chemical structure).^{30,73} These global MHD simulations show that advection has no specified direction in various disk regions, and in each location goes both inward and outward. The corresponding turbulent velocity of the gas V_{turb} depends on the viscosity parameter α and scales with it somewhere between linear and square-root dependence, $\alpha < V_{\text{turb}}/c_s < \sqrt{\alpha}$; here, c_s is the sound speed. The calculated α -viscosity stresses have values in a range of 10^{-4} and 10^{-2} in the midplane and the molecular layer, respectively, and rise steeply to transonic values of ~ 0.5 in the disk atmosphere. Similar values of microturbulent velocities in the disk of DM Tau have been derived,¹⁴⁵ using the heavy molecule CS to distinguish between Keplerian, thermal, and nonthermal line components. Hughes et al. (2011)³³⁷ have used the CO molecule and estimated turbulent velocities in disks around the Sun-like star TW Hya and the hotter, twice as massive star HD 163296, with about 10% and 40% of the sound speed, respectively.

Given this large body of empirical evidence, for decades modelers have investigated the impact of various dynamical processes on the chemical evolution of gas and solids in the solar nebula and protoplanetary disks. Models of the early solar nebula with radial transport by advective flows have been developed,^{60,242,250,251} with a simple 1D analytical disk model and passive tracers. The 2D radial mixing of gaseous and solid water in the inner nebula has been studied.³³⁸ Bauer et al.²⁴⁶ have investigated the influence of radial transport on the gas-phase C-, H-, N-, O-chemistry driven by dust destruction and evaporation of ices. The major result is that radial transport enriches the outer, $r > 10$ AU regions with methane and acetylene produced by oxidation of carbon dust at $r \lesssim 1$ AU, as was observed in comets Hyakutake and Hale-Bopp. In a recent study of that kind, Tscharnatur and Gail (2007)⁶⁵ have considered a 2D disk chemo-hydrodynamical model in which global circulation flow patterns exist, transporting disk matter outward in the disk midplane and inward in elevated disk layers. They found that gas-phase species produced by warm neutral-neutral chemistry in the inner region can be transported into

the cold outer region and freeze-out onto dust grain surfaces. We should note that global 3D MHD simulations do not show any evidence for such meridional circulation patterns,^{30,73} which would imply that the meridional transport of molecules does not occur.

Studies of the chemistry coupled to the dynamics in protoplanetary disks is a relatively recent research field. Aikawa et al. (1999)²⁰⁷ have used an isothermal hydrostatic α -disk model⁶⁹ with an accretion rate of $\dot{M} = 10^{-8} M_{\odot} \text{ yr}^{-1}$, and modeled chemical evolution with inward accretion. They found that within 3 Myr one can transport a parcel of gas from 400 to 10 AU. This inward transport enhances concentrations of heavy hydrocarbons at $\lesssim 20$ AU, whereas methane remains a dominant hydrocarbon in the outer disk region. This also leads to the simultaneous existence of reduced (e.g., CH₄) and oxidized (e.g., CO₂) ices, similar to what is observed in comets.

Ilgner et al. (2004)⁶¹ have used a steady α -disk model and considered 1D vertical mixing using a turbulent eddy turnover description³³⁹ and a 1D Lagrangian description for advective transport (from 10 to 1 AU). They found that mixing lower vertical abundance gradients and that local changes in species concentrations due to mixing can be radially transported by advection. They have concluded that diffusion does not affect disk regions dominated by gas–grain kinetics, while it enhances abundances of simple gas-phase species like O, SO, SO₂, CS, etc. Later, Ilgner and Nelson (2006)⁵⁵ have studied the ionization structure of inner disks ($r < 10$ AU), considering vertical mixing and other effects like X-ray flares, various elemental compositions, etc. They found that mixing has no profound effect on electron concentration if metals are absent in the gas since recombination time scales are faster than dynamical time scales. However, when $T \gtrsim 200$ K and alkali atoms are present in the gas, chemistry of ionization becomes sensitive to transport, such that diffusion may reduce the size of the turbulent-inactive disk “dead” zone.

Willacy et al. (2006)⁶² have attempted to systematically study the impact of disk viscosity on evolution of various chemical families. They used a steady-state α -disk model similar to that of Ilgner et al. (2004) and considered 1D-vertical mixing in the outer disk region with $r > 100$ AU. They found that vertical transport can increase column densities (vertically integrated concentrations) by up to 2 orders of magnitude for some complex species. Still, the layered disk structure was largely preserved even in the presence of vertical mixing. Semenov et al. (2006)²⁷⁸ and Aikawa (2007)⁶³ have found that turbulence can transport gaseous CO from the molecular layer down toward the cold midplane where it otherwise remains frozen out, which may explain the large amount of cold ($\lesssim 15$ K) CO gas detected in the disk of DM Tau.¹³⁷ Hersant et al. (2009)⁶⁶ have studied various mechanisms to retain gas-phase CO in very cold disk regions, including vertical mixing. They found that photodesorption in upper, less obscured molecular layer greatly increases the gas-phase CO concentration, whereas the role of vertical mixing is less important.

Later, in Woods and Willacy (2007)²¹⁰ the formation and destruction of benzene in turbulent protoplanetary disks at $r \lesssim 35$ AU has been investigated. These authors found that radial transport allows efficient synthesis of benzene at $\lesssim 3$ AU, mostly due to ion–molecule reactions between C₃H₃ and C₃H₄⁺ followed by grain dissociative recombination. The resulting concentration of C₆H₆ at larger radii of 10–30 AU is increased by turbulent diffusion up to 2 orders of magnitude. In a similar study, Nomura et al. (2009)²⁷⁵ have considered inner disk

model with radial advection ($\lesssim 12$ AU). They found that the molecular concentrations are sensitive to the transport speed, such that in some cases gaseous molecules are able to reach the outer, cooler disk regions where they should be depleted. This increases the production of many complex or surface-produced species such as methanol, ammonia, hydrogen sulfide, acetylene, etc.

Heinzeller et al. (2011)⁶⁷ have studied the chemical evolution of a protoplanetary disk with radial viscous accretion, vertical mixing, and a vertical disk wind (in the atmosphere). They used a steady-state disk model with $\alpha = 0.01$ and $\dot{M} = 10^{-8} M_{\odot} \text{ yr}^{-1}$. They found that mixing lowers concentration gradients, enhancing abundances of NH₃, CH₃OH, C₂H₂, and sulfur-containing species. They concluded that the disk wind has a negligible effect on chemistry, while the radial accretion changes molecular abundances in the midplane, and the vertical turbulent mixing enhances abundances in the intermediate molecular layer.

A detailed study of the effect of 2D radial-vertical mixing on gas–grain chemistry in a protoplanetary disk has been performed.⁶⁸ These authors used the α -model of a ~ 5 Myr DM Tau-like disk coupled to the large-scale gas–grain chemical code “ALCHEMIC”.³⁰³ To account for production of complex molecules, an extended set of surface processes was added. A constant value of the viscosity parameter $\alpha = 0.01$ was assumed, and the diffusion coefficient was calculated as

$$D_{\text{turb}}(R, z) = \nu(R, z)/Sc = \alpha c_s(R)H(R)/Sc \quad (3)$$

where Sc is the Schmidt number describing the efficiency of turbulent diffusivity.^{72,340}

In this study it was shown that the higher the ratio of the characteristic chemical time scale to the turbulent transport time scale for a given species, the higher the probability that its concentration is affected by dynamics. Consequently, turbulent transport changes the abundances of many gas-phase species and particularly ices. Vertical mixing is more important than radial mixing, mainly because radial temperature and density gradients in disks are weaker than vertical ones. The simple molecules not responding to dynamical transport include C₂H, C⁺, CH₄, CN, CO, HCN, HNC, H₂CO, OH, as well as water and ammonia ices. The species sensitive to transport are carbon chains and other heavy species, in particular sulfur-bearing and complex organic molecules (COMs) frozen onto the dust grains. This is because mixing allows ice-coated grains to be steadily transported into warmer inner disk regions where efficient surface recombination reactions proceed. In the warm molecular layer these complex ices evaporate and return to the gas phase. It was reconfirmed that mixing does not completely smear out the vertical layered structure of protoplanetary disks (see also refs 62, 67, 207).

Finally, several promising, particularly sensitive, detectable tracers of dynamical processes in protoplanetary disks were identified. These are the ratios of concentrations of CO₂, O₂, SO, SO₂, C₂S, C₃S, and organic molecules to that of CO and water ice (see Table 4).

4. WATER AND HYDROXYL MOLECULES IN PROTOPLANETARY DISKS

The chemistry of water in protoplanetary disks and the conversion of water vapor into molecular ice are directly linked to the origin of water on Earth and the formation of giant planets beyond the snow line. This line defines the location in the disk where water vapor freezes out to molecular ice. The

Table 4. Detectable Tracers of Turbulent Mixing

insensitive	hypersensitive
CO	heavy hydrocarbons (e.g., C ₆ H ₆)
H ₂ O ice	C ₂ S
	C ₃ S
	CO ₂
	O ₂
	SO
	SO ₂
	OCN
	complex organics (e.g., HCOOH)

position of the snow line depends on the pressure and temperature in the disk and, therefore, on the disk mass and heating processes. For the solar nebula it is generally assumed that the snow line was located somewhere between 2 and 3 AU from the Sun. The planets Jupiter, Saturn, Uranus, and Neptune all formed beyond the snow line (see section 3.3) and are enriched in volatiles relative to the Sun.³⁴¹ In general, giant planets in other planetary systems are thought to form beyond the snow line.³⁴² It is very likely that the volatiles were trapped in molecular ices when accreted onto the planets. The term “volatiles” comprises all material with low melting and condensation temperatures (gases or molecular ices) in contrast to “refractory” materials such as metallic iron and silicates. Water and carbon monoxide are by far the most abundant simple “volatile” molecules, with NH₃, CH₄, and CO₂ as other important ices.

Because of a large reservoir of volatiles in the outer solar nebula, the two giant planets Jupiter and Saturn could first form massive solid cores and then gravitationally attract giant H–He gas envelopes. The two outermost planets in the solar system, Uranus and Neptune, are largely composed of molecular ices such as water, methane, and ammonia, and are, therefore, called the ice giants. Water, CO, and CO₂ are the most abundant molecular ices in comets with small admixtures of methane and ammonia and other minor components (e.g., C₂H₆).³⁴³

Two main processes have been discussed as explanation for the source of water on Earth: (i) delivery of hydrous silicate grains to Earth and outgassing of volatiles by volcanoes, wet proto-Earth formation;³⁴⁴ and (ii) delivery of water by certain classes of comets and asteroids, dry proto-Earth formation.²²¹ Arguments against delivery of water by hydrous silicates come from the low water content in anhydrous meteoritic silicates and the nondetection of spectral features of hydrous silicates in infrared disk spectra. A key to our understanding of the origin of water on Earth is its D/H ratio with a mean ocean water value of 1.55×10^{-4} , which is much larger than the primordial value of the interstellar medium (1.5×10^{-5}), see Figure 7. This enhanced D/H ratio points to mass fractionation during chemical reactions at low temperatures (see section 5). Measurements of D/H ratios for asteroids and comets indicate that a mixture of these bodies delivered water to Earth.^{345,346}

We should note that most of the water, at least in the outer regions of protoplanetary disks, is frozen out on dust grain surfaces.^{299,347} There is growing evidence that the water ices may already have been formed in the prestellar and protostellar phases. Visser et al. (2009)³¹⁰ found that water remains in the solid phase everywhere during the infall and disk formation phases, and evaporates within ~ 10 AU of the star. In contrast, pure CO ice evaporates during the infall phase and is reformed in those parts of the disk that cool below the CO freeze-out

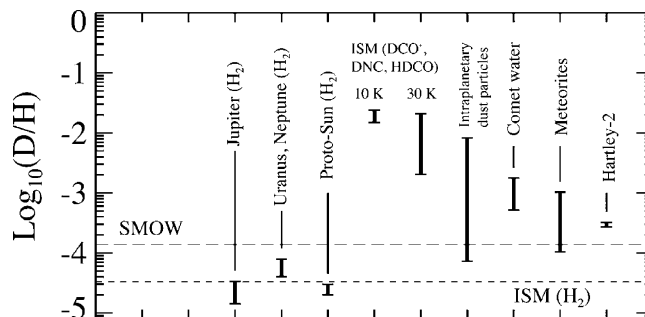


Figure 7. Observed D/H ratio for H₂O in various astrophysical environments ranging from the interstellar medium to comets and the Earth's ocean water. The “ISM (H₂)” (dashed line) represents the HD/H₂ in dense cold ISM. “SMOW” (long dashed line) denotes the HDO/H₂O ratio in the Vienna standard mean ocean water model. Data derived from ref 34.

temperature of ~ 20 K. These authors also found that mixed CO:H₂O ices will keep some solid pristine CO above this temperature threshold and may explain the presence of CO in comets.

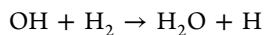
Hot water (≈ 500 – 1000 K) has been discovered in the inner regions of protoplanetary disks (0.1–10 AU) around young solar-mass T Tauri stars by ground-based mid-infrared spectroscopy and infrared observations with the Spitzer Space Observatory,^{158,159,161,167,169,212,348,349} see Figure 4. Water is a highly asymmetric molecule with a rich infrared spectrum produced by transitions between energy levels characterized by 3 quantum numbers J , K_A , and K_B . The infrared emission of the water molecules comes predominantly from a warm disk surface layer.

Water exists in two spin states: ortho-H₂O with total nuclear spin of unity and para-H₂O with total nuclear spin of zero. Either direct radiative or collisional transitions between ortho- and para-H₂O energy levels are not allowed, and the ortho-to-para ratio can only be modified by chemistry by proton exchange. The ortho-to-para ratio in the high-temperature limit is regulated by spin statistics resulting in a ratio 3:1. Water formation on cold grain surfaces may allow lower ortho-to-para ratios through equilibration at the dust temperature.¹⁵³

In contrast to the observations of rich water-dominated infrared spectra from disks around T Tauri stars, water has not been detected in the inner disks around the more massive and luminous Herbig Ae/Be stars.²¹³ A likely explanation of this observational finding is the photodissociation of hot water by the stronger ultraviolet radiation field of these stars. In fact, it has been demonstrated that the H₂O emission from the disk around the young eruptive star EX Lupi is variable as a likely consequence of the changing ultraviolet radiation field.³⁴⁹

Cooler water emission (at temperatures of ≈ 100 – 500 K) has been discovered with the Herschel Space Observatory in the far-infrared spectra of disks around T Tauri stars^{151,152} and in a small number of Herbig Ae/Be stars by line stacking.^{149,152} It has been directly detected in the disk around the Herbig Ae star HD 163296, which is enshrouded by a flat disk with settled dust.¹⁵⁰ Overall, disks around Herbig Ae/Be stars have higher OH/H₂O abundance ratios across the inner disks than T Tauri stars.

Above a temperature of ≈ 300 K water should be the dominant oxygen-containing component in the gas, assuming solar-elemental abundances.^{350,351} Water is formed rapidly by two neutral–neutral reactions in the warm gas:



An extensive discussion of the relevant rate constants for these reactions can be found here.^{350–352} At temperatures lower than a few 100 K, ion-neutral reactions become an important channel for water production. The key molecular ion H_3^+ will react with atomic oxygen, producing H_3O^+ which recombines via a number of dissociative reaction channels, among them a reaction to H and H_2O . In the midplane of the outer disks, water is frozen out on dust grains. The water molecules can be released by UV photodesorption²⁹⁹ in intermediate layers of the disk, and water gets photodissociated in the upper disk atmospheres. The complicated interplay between grain evolution, grain surface chemistry and freeze-out, photodesorption and photodissociation, and radial and vertical mixing processes will regulate the abundance of water in its different phases in the outer disk.^{71,98,216,353}

The discovery of the ground-state rotational emission of both spin isomers of water from the outer disk around the star TW Hya with Herschel's high-resolution spectrometer HIFI¹⁵³ provided strong constraints on the water vapor abundance in the outer disk with a layer of maximum water abundance of $\approx 10^{-7}$ relative to H_2 . Above this layer, water gets photodissociated; below, it freezes. The observations allowed the determination of the ortho-to-para ratio (OPR). The derived value of 0.77 ± 0.07 is much lower than the equilibrium value of 3 and indicates that grain surface reactions and photodesorption play an important role in producing the observed water vapor. This value is also lower than the OPR H_2O ratios for solar system comets, ranging from 2 to 3.^{354–358} If one interprets the OPR values in terms of a spin temperature, as is often done in the literature, and equates this temperature with the physical temperature of the dust on which water ice has formed, this would indicate that water in TW Hya has formed at lower temperatures (10–20 K) than in comets (~ 50 K).¹⁵³

5. DEUTERIUM CHEMISTRY IN DISKS

Among the most important findings related to the chemical evolution in the early solar nebula is isotopic fractionation. Many cometary and meteoritic materials show anomalous isotopic enrichment in such elements as oxygen, carbon, nitrogen, and sulfur.^{318,320,359–361} In particular, amino acids found in carbonaceous meteorites^{362,363} and recently discovered glycine in cometary samples returned by the Stardust mission³⁶⁴ show extraterrestrial isotopic signatures. The composition of terrestrial minerals, water, and rocks on Earth retains an imprint of the rate differences at which fractionation has occurred.

Deuterium fractionation is a nonequilibrium process sensitive to temperature and thermal history of an environment. Formed right after the Big Bang, with an initial elemental ratio of D/H $\approx 310^{-5}$, only half of this deuterium has survived until today, mostly in the form of the HD molecule (the other half was burned in stellar interiors).^{365,366} However, at low temperatures, $T \lesssim 20$ –80 K, part of the deuterium from HD can be redistributed into other molecules by ion–molecule and surface chemistry, resulting in higher molecular D/H ratios than the value of 1.5×10^{-5} . In Figure 7 we show D/H ratios measured for several molecules (H_2 , H_2O , HCN, HCO^+ , H_2CO , etc.) in planets of the solar system, comets, asteroids, interplanetary dust particles, and the standard mean ocean water (SMOW).

The D/H ratio for H_2 in the diffuse interstellar medium (ISM) of $\approx 3 \times 10^{-5}$ is also indicated. As can be clearly seen, all gas and icy giants as well as the (proto-)Sun have the cosmic elemental D/H ratios for H_2 similar to the ISM H_2 D/H value. These objects have warm interiors and high densities to redistribute deuterium among chemical species at nearly equilibrium conditions. In contrast, cold ISM environments like prestellar cores or warm protostellar envelopes have D/H ratios for DCO^+ , DCN, HDCO, etc. that are higher than the cosmic value by factors of ~ 100 –300.^{367–369} Part of this parental, highly deuterium-enriched cloud core matter ends up in a protoplanetary disk where it is incorporated into meteorites, asteroids, and comets. The D/H ratios measured in meteorites and observed in long-period comets from the Oort cloud are also enhanced by factors of at least 10–30 compared to the elemental D/H ratio,³⁷⁰ which is lower than the molecular ISM values. As discussed in section 4, water has likely been delivered to Earth by bodies from more distant parts of the solar system as the planetesimals out of which Earth has formed were presumably dry. Not surprisingly, the Earth water bears signature of this exogenous delivery scenario by showing about a 10 times enhanced D/H ratio in ocean's water, $\approx 1.6 \times 10^{-4}$, compared to the elemental ISM D/H value. As the Oort-family long-period comets all show 2–3 times higher $\text{HDO}/\text{H}_2\text{O}$ ratios, whereas carbonaceous chondrites have about the Earth $\text{HDO}/\text{H}_2\text{O}$ value, it was argued that water came to Earth with asteroids, not comets. However, the recent discovery of nearly Earth's ocean water D/H signature in a Jupiter-family, short-period comet Hartley-2³⁴⁶ has reignited this discussion.

What happens with deuterated species in transition from the cold conditions of the ISM to the warm conditions in the planet-forming region can be best understood by studying deuterium chemistry in protoplanetary disks. Several deuterated molecules have been detected in protoplanetary disks, with abundances much higher than the cosmic elemental D/H ratio of 1.5×10^{-5} . The measured D/H ratios of DCN and DCO^+ in the disk around TW Hya are about 1–10%.³⁷¹ Öberg et al. (2012)¹⁸¹ have found that the DCO^+ column density increases outward, whereas DCN is more centrally peaked. This suggests different fractionation pathways, with DCN forming at higher temperatures than DCO^+ . The derived DCN/HCN ratio is similar to that of $\text{DCO}^+/\text{HCO}^+$, ~ 0.017 . A smaller $\text{DCO}^+/\text{HCO}^+$ value, 4×10^{-3} , has been measured in the disk of DM Tau.¹⁷⁸

The observed overabundance of deuterated species in the cold ISM and protoplanetary disks is due to isotopic deuterium fractionation. This process is related to the zero-point vibrational energy difference for the isotopically substituted molecules, implying a temperature barrier for a backward reaction at low temperatures. The main isotope exchange reaction involves isotopologues of H_3^+ and H_2 , and is effective at $T \lesssim 10$ –30 K: $\text{H}_3^+ + \text{HD} \rightleftharpoons \text{H}_2\text{D}^+ + \text{H}_2 + 232$ K,^{372,373} followed by similar reactions with higher D-isotopologues. This leads to accumulation of H_2D^+ , which further transfers D into other molecules by ion–molecule reactions.^{374–376} For example, the dominant formation pathway to produce DCO^+ is via ion–molecule reactions of CO with H_2D^+ . In disks it results in a DCO^+ to HCO^+ ratio that should increase with radius due to the outward decrease of temperature, as actually observed. Deuterium fractionation initiated by the H_3^+ isotopologues is particularly effective at low temperatures in disk midplanes, where CO and other molecules that destroy the H_3^+ isotopologues are severely frozen out.

On the other hand, the H_3^+ isotopologues can dissociatively recombine with electrons, producing a flux of atomic H and D. In the cold, dense regions such as outer disk midplanes H and D atoms can stick to dust grains and react with ices such as CO, O, C, and form multideuterated complex species (isotopologues of, e.g., H_2CO , CH_3OH , H_2O). Moreover, laboratory experiments have demonstrated that on dust surfaces a substitution of a proton by deuteron in H-bearing species can occur, accelerating deuterium enrichment of complex ices.^{377–380}

Recently, it has been realized that the ortho/para ratio of H_2 and other species can lower the pace of deuterium fractionation.^{381,382} The internal energy of ortho- H_2 is higher than that of para- H_2 , which helps to overcome the backward reaction of deuterium enrichment. For example, the backward endothermic reaction between ortho- H_2 and H_2D^+ can proceed far more rapidly at low temperatures of 10 K than the corresponding reaction involving its para form. Consequently, it results in a lower degree of deuterium fractionation in a medium having a sufficient amount of ortho- H_2 .³⁸¹

Other important fractionation reactions are effective at higher temperatures (up to 70–80 K), and are particularly relevant for inner, warmer disk regions: $\text{CH}_3^+ + \text{HD} \rightleftharpoons \text{CH}_2\text{D}^+ + \text{H}_2 + 390 \text{ K}$ ³⁸³ and $\text{C}_2\text{H}_2^+ + \text{HD} \rightleftharpoons \text{C}_2\text{HD}^+ + \text{H}_2 + 550 \text{ K}$.³⁸⁴ Both reactions produce DCN by the following ion–molecule reaction $\text{N} + \text{CH}_2\text{D}^+ \rightarrow \text{DCN}^+$, followed by protonation by H_2 and dissociative recombination.³⁸⁵ Compared to DCO^+ , DCN can thus be formed at warmer temperatures and reside closer to the central star in protoplanetary disks, exactly as observed in the TW Hya disk.¹⁸¹

These observational findings in protoplanetary disks have been compared to theoretical studies. Aikawa and Herbst (1999)²⁶⁹ have studied deuterium chemistry in the outer regions of protoplanetary disks with an 1D accretion flow, using a collapse model to set up the initial molecular concentrations. They have found that the molecular D/H ratios are enhanced with regard to the protosolar values, and that the ratios at ~30 AU agree reasonably well with the D/H ratios observed in comets. This advocates for *in situ* deuterium fractionation in the solar nebula, so that comets may not necessarily be composed of primordial, unprocessed interstellar matter. Willacy (2007)²⁷² and Willacy and Woods (2009)²⁷³ have studied deuterium chemistry in outer and inner disk regions, respectively. They found that the D/H ratios observed in comets may partly originate from the parental molecular cloud and partly be produced in the disk. They concluded that the D/H ratios of gaseous species are more sensitive to deuterium fractionation processes in disks due to rapid ion–molecule chemistry compared to the deuterated ices, whose D/H values are regulated by slow surface chemistry and are imprints of the cold conditions of the prestellar cloud.

The previous discussion shows that fractionation processes occur both in the prestellar cloud phase and in the protoplanetary disk phase. This complicates the use of D/H ratios as a clean “tool” to distinguish between the contribution from prestellar chemistry and disk chemistry to the molecular composition of disks.

6. COMPLEX ORGANIC MOLECULES

One of the most exciting questions in astrochemistry are (1) the exact form in which carbon-based materials exist under space conditions,³⁸⁶ and (2) how and which prebiotic life-building blocks can survive the process of star and planet

formation. In the ISM solid carbonaceous compounds can be identified through numerous aromatic (C–C) and aliphatic (C–H) stretching and bending modes at infrared wavelengths^{387–389} and a strong ultraviolet resonance,^{390–392} and are believed to take the form of hydrogenated amorphous carbon (nanoparticles), with various fraction of H as well as sp^2 and sp^3 carbon atoms,^{389,393} or occur as large PAHs.^{386,392} About 1–10% (depending on far-UV/X-ray irradiation) of all cosmic carbon is locked in PAHs.^{394,395} A small, $\lesssim 3\text{--}4\%$ fraction of carbon condenses out as (nano)diamond particles that are found as presolar grains in meteorites.³⁵⁹ Also, some elemental C is locked in tightly bound silicon carbide (SiC) grains, which are mostly of stardust origin.^{396,397}

Many different amino acids and other complex organics (in insolvable and solvable forms) were present in the early solar system, as found through detailed mass-spectrometry and mineralogical and petrological analysis of primitive carbonaceous chondrites³⁶² and interplanetary dust particles.³⁹⁸ Analysis of the cometary dust sampled by the Giotto spacecraft in the Halley comet showed the presence of the so-called organic “CHON” particles (which are large molecules composed of multiple C, H, O, and N atoms³⁹⁹). The recent identification of glycine in the Stardust cometary dust samples³⁶⁴ provides strong evidence that comets may have an organically rich composition, a fact which is also supported by their extremely low albedos. These findings were also interpreted as indication that initial carbonaceous materials of the ISM could have been almost entirely chemically reprocessed into complex organics prior to or during the formation of the inner solar system, within several million years.¹⁹⁶ Indeed, the discovery of highly deuterated amino acids in meteoritic materials (as well as other isotopic anomalies in C, N, and O) implies that their (at least, initial) synthesis occurred under very cold and dark conditions characteristic of dense prestellar molecular clouds.^{325,400,401} This hypothesis is supported by the detection of complex organic molecules (COMs) such as methanol (CH_3OH), acetaldehyde (CH_3CHO), dimethyl ether (CH_3OCH_3), methyl formate (CH_3OCHO), and ketene (CH_2CO), etc., in the gas phase in cold, young, low-mass prestellar cores.^{402,403} Glycolaldehyde and formamide (NH_2CHO), the simplest amide, a key species in the synthesis of amino acids and metabolic molecules, have also been recently detected in envelopes of solar-type protostars.^{404–406}

On the other hand, COMs could also have formed at the verge of planet formation in the heavily irradiated, warm inner regions of the solar nebula by endothermic chemistry from simple species such as CO, N₂, OH, and H₂.^{322,323} The formation of protoplanetary disks from their parental molecular clouds is associated with strong shocks that can reprocess the gas and some ices.⁴⁰⁷ The newly produced COMs can either be trapped in the ices and become incorporated in comets or return into the gas phase by thermal desorption, UV-photodesorption, or heating triggered by cosmic ray particles and X-rays.^{237,408–410} Also, the Fischer–Tropsch catalysis converts CO and H₂ into hydrocarbons at appropriate temperatures ($T \gtrsim 1\,000 \text{ K}$) in the presence of metallic surfaces. In a similar manner, the catalytic Haber–Bosch synthesis produces ammonia from N₂ and H₂.⁴¹¹ The overall efficiency of both these processes depends on the properties of the metallic surfaces (e.g., poisoning by other materials, refractory ice coatings, topology) and the fraction of metallic iron and nickel incorporated in silicates and left in their metallic

(or oxidized) forms. The appropriate conditions for such synthesis must have existed in the very inner, sub-AU, accretion-heated regions of the early solar nebula and may exist in other actively accreting protoplanetary disks.⁴¹² Also, in this hot region PAHs are gradually destroyed by neutral–neutral reactions with barriers with H, OH, and O, resulting in high concentrations of acetylene (C_2H_2) and, later, CO, CO_2 , and CH_4 .⁴¹³

The most plausible scenario of the synthesis of COMs is that the first-generation, simpler organic molecules have been synthesized already during the pre-disk, cold cloud phase, followed by production of second-generation, more complex organics inside warm, irradiated disk regions. The further growth in their complexity could have been enabled by aqueous alteration inside large, radiogenically heated asteroids.

Despite the variety of interstellar COMs, only formaldehyde (H_2CO), C_2H , C_3H_2 , HCN, HNC, and HC_3N and a few other inorganic species have been detected and spatially resolved with (sub)millimeter interferometers in the outer regions ($r \gtrsim 50–200$ AU) of several nearby protoplanetary disks.^{35,47,50,141,143,144,147,148,414} The ground-based search for simple gas-phase organic species such as methanol and formic acid in disks has so far been unsuccessful. On the other hand, simple organic ices, like HCOOH ice, have been identified in the Spitzer infrared spectra of the envelopes of low-mass class I/II objects.⁴¹⁵ The main reasons for the lack of detections of COMs in protoplanetary disks are the low masses and small sizes of these objects, and the severe depletion of these heavy species onto dust surfaces in outer cold regions of the disks (see Figure 5). Formaldehyde and formic acid are just precursors for the synthesis of other complex organic ices via slow photoprocessing, forming reactive radicals in the icy mantles, which can further recombine with each other at appropriate conditions.^{416–419} Dynamical transport from cold to warm/irradiated regions in protoplanetary disks can also lead to efficient desorption of heavy ices (see section 3.5). A rich organic chemistry occurring in the inner warm disk regions has been confirmed with infrared spectroscopy by Spitzer. Detected species include CO, CO_2 , C_2H_2 , CN, and HCN, which reside in the warm gas, $T \gtrsim 200–1000$ K.^{158–160,162–165,171,348}

The importance of dynamical transport for the synthesis of COMs in the early solar nebula has been studied in ref 68 (see section 3.5 for a brief description of their model). The main results are presented in Figure 8. The plot shows distributions of absolute concentrations and vertically integrated column densities of HCOOH, HCOOH ice, CH_3OH , HNCO, HNCO ice, CH_3CHO , CH_3CHO ice, and CH_2CO calculated with a quiescent and a rapid turbulent mixing model of the solar nebula. In the dynamically quiescent model the abundance distributions of gaseous species have a layered structure, with very narrow layers of peak concentrations located at $\approx 0.8–1$ pressure scale heights. Abundances of complex ices reach peak values at either the bottom of the molecular layer (HNCO ice, HCOOH ice) or in the inner warm midplane (CH_3CHO ice, HCOOH ice). The overall pattern is easily explained by photoevaporation of heavy COM ices, which in the gas phase become susceptible to ionizing far-UV/X-ray radiation and are rapidly photodissociated. On the other hand, dynamical transport facilitates the synthesis of COMs by transporting icy grains toward warm or irradiated disk regions, where heavy reactive radicals are formed upon CRP/X-ray irradiation of ices, followed by surface recombination when they become mobile at $T \gtrsim 30–50$ K.

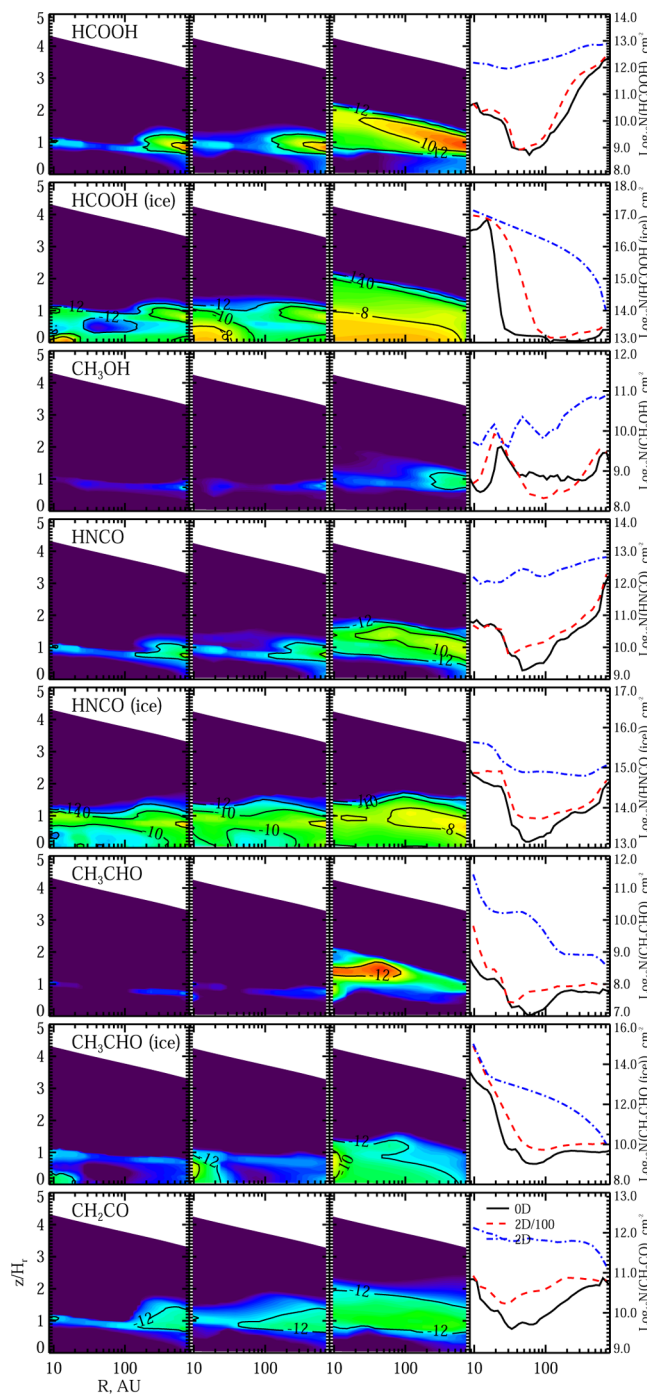


Figure 8. Radial and vertical variations of abundances and column densities of complex organic molecules in the DM Tau disk at 5 Myr (top to bottom, left columns). The log of relative abundances (with respect to the total number of hydrogen nuclei) of HCOOH, HCOOH ice, CH_3OH , HNCO, HNCO ice, CH_3CHO , CH_3CHO ice, and CH_2CO . Results for the three disk models are shown: (1) laminar chemistry, (2) the slow 2D-mixing chemistry ($Sc = 100$), and (3) the fast 2D-mixing chemistry with $Sc = 1$. The corresponding vertical column densities (abundances integrated in the vertical direction) are shown in the right part of the figure. Reprinted with permission from ref 68. Copyright 2011 American Astronomical Society.

We list the most important reactions for the evolution of HCOOH, HCOOH ice, CH_3OH , HNCO, HNCO ice, CH_3CHO , CH_3CHO ice, and CH_2CO in the solar nebula and protoplanetary disk midplanes and molecular layers in

Table 5. The chemical evolution of formic acid (HCOOH) begins with the dissociative recombination of CH_3O_2^+ , which is

Table 5. Key Chemical Processes: Organic Species

reaction	$\alpha \text{ [cm}^3 \text{s}^{-1}\text{]}$	β	$\gamma \text{ (K)}$
CH_2CO ice + $h\nu_{\text{CRP}}$ → CH_2 ice + CO ice	9.15 (2)	0	0
CH_2CO ice + $h\nu_{\text{CRP}}$ → C_2 ice + H_2O ice	4.07 (2)	0	0
CH_3CHO ice + $h\nu_{\text{CRP}}$ → CH_3 ice + HCO ice	5.25 (2)	0	0
CH_3CHO ice + $h\nu_{\text{CRP}}$ → CH_4 ice + CO ice	5.25 (2)	0	0
CH_3OH ice + $h\nu_{\text{CRP}}$ → CH_3 ice + OH ice	1.50 (3)	0	0
CH_3OH ice + $h\nu_{\text{CRP}}$ → H_2CO ice + H_2 ice	3.17 (3)	0	0
$\text{C}_2\text{H}_5\text{OH}$ ice + $h\nu_{\text{CRP}}$ → CH_3CHO ice + H_2 ice	6.85 (2)	0	0
HCOOH ice + $h\nu_{\text{CRP}}$ → CO_2 ice + H ice + H ice	6.50 (2)	0	0
HCOOH ice + $h\nu_{\text{CRP}}$ → HCO ice + OH ice	2.49 (2)	0	0
HNCO ice + $h\nu_{\text{CRP}}$ → NH ice + CO ice	6.00 (3)	0	0
CH_3OH ice + UV → H_2CO ice + H_2 ice	0.72 (-9)	0	1.72
$\text{C}_2\text{H}_5\text{OH}$ ice + UV → CH_3CHO ice + H_2 ice	0.13 (-9)	0	2.35
HCOOH ice + UV → HCO ice + OH ice	0.28 (-9)	0	1.80
$\text{HNCO} + h\nu_{\text{CRP}} \rightarrow \text{NH} + \text{CO}$	6.00 (3)	0	0
$\text{CH}_3\text{CHO} + \text{UV} \rightarrow \text{CH}_3\text{CHO}^+ + e^-$	0.26 (-9)	0	2.28
$\text{CH}_3\text{CHO} + \text{UV} \rightarrow \text{CH}_4 + \text{CO}$	0.34 (-9)	0	1.52
$\text{CH}_3\text{CHO} + \text{UV} \rightarrow \text{CH}_3 + \text{HCO}$	0.34 (-9)	0	1.52
$\text{HCOOH} + \text{UV} \rightarrow \text{HCOOH}^+ + e^-$	0.17 (-9)	0	2.59
$\text{HCOOH} + \text{UV} \rightarrow \text{HCO} + \text{OH}$	0.28 (-9)	0	1.80
$\text{CH}_2\text{CO} + \text{grain} \rightarrow \text{CH}_2\text{CO}$ ice			
$\text{HCOOH} + \text{grain} \rightarrow \text{HCOOH}$ ice			
$\text{HNCO} + \text{grain} \rightarrow \text{HNCO}$ ice			
$\text{CH}_3\text{CHO} + \text{grain} \rightarrow \text{CH}_3\text{CHO}$ ice			
$\text{CH}_3\text{OH} + \text{grain} \rightarrow \text{CH}_3\text{OH}$ ice			
HNCO ice → HNCO	2.85 (3)		
CH_2CO ice → CH_2CO	2.20 (3)		
CH_3CHO ice → CH_3CHO	2.87 (3)		
H ice + CH_2OH ice → CH_3OH ice			
H ice + HC_2O ice → CH_2CO ice			
H ice + OCN ice → HNCO ice			
OH ice + CH_3 ice → CH_3OH ice			
OH ice + HCO ice → HCOOH ice			
$\text{HCOOH} + \text{H}^+ \rightarrow \text{HCOOH}^+ + \text{H}$	0.28 (-8)	-0.50	0
$\text{HNCO} + \text{H}^+ \rightarrow \text{NH}_2^+ + \text{CO}$	0.15 (-7)	-0.50	0
$\text{CH}_3\text{CHO} + \text{H}_3^+ \rightarrow \text{CH}_3\text{CH}_2\text{O}^+ + \text{H}_2$	0.62 (-8)	-0.50	0
$\text{CH}_3\text{CHO} + \text{HCO}^+ \rightarrow \text{CH}_3\text{CH}_2\text{O}^+ + \text{CO}$	0.25 (-8)	-0.50	0
$\text{HCOOH} + \text{H}_3^+ \rightarrow \text{HCO}^+ + \text{H}_2\text{O} + \text{H}_2$	0.23 (-8)	-0.50	0
$\text{HCOOH} + \text{HCO}^+ \rightarrow \text{CH}_3\text{O}_2^+ + \text{CO}$	0.13 (-8)	-0.50	0
$\text{O} + \text{C}_2\text{H}_5 \rightarrow \text{CH}_3\text{CHO} + \text{H}$	0.13 (-9)	0	0
$\text{OH} + \text{H}_2\text{CO} \rightarrow \text{HCOOH} + \text{H}$	0.20 (-12)	0	0

produced by radiative association of HCO^+ and H_2O , and by ion–molecule reaction of methane with ionized molecular oxygen. HCOOH is destroyed by photodissociation and photoionization, and removed from the gas due to depletion onto dust grains at $T \lesssim 100$ K. Then, HCOOH ice forms, which is destroyed by far-UV photons generated in the disk by CRP (or the attenuated stellar far-UV photons in the disk

molecular layer). The surface and gas-phase formation of HCOOH through the neutral–neutral reaction of OH and H_2CO is only a minor channel. Gas-phase methanol is synthesized by surface recombination of H and CH_2OH as well as frozen OH and CH_3 (at $T \gtrsim 30$ K) followed by evaporation of the methanol ice. The main removal pathways for CH_3OH are accretion onto the dust surfaces in the disk regions with $T \gtrsim 100$ K, photodissociation, and ionization.

We now will discuss the chemistry of the isocyanic acid (HNCO) in detail because this molecule is a key molecule in the chemical processes on dust surfaces⁴²⁰ and an important diagnostic species.⁴²¹ The production of HNCO is also dominated by surface reactions. It can reach the gas phase either by evaporation of HNCO ice at $T \lesssim 50$ –60 K or by direct recombination of surface H and OCN (by chemisorption). The major destruction gas-phase pathways for HNCO are accretion onto the dust grain surfaces. HNCO ice is produced by a surface reaction involving H and OCN and is destroyed by far-UV photons. Similarly, the chemistry of acetaldehyde (CH_3CHO) begins with the surface recombination of CH_3 and HCO ices followed by desorption to the gas phase at $T \lesssim 60$ K. It is destroyed by photodissociation. Gas-phase ethenone (CH_2CO) is produced via neutral–neutral reactions of atomic O with C_2H_3 , and direct surface recombination of the H and HC_2O ices. Evaporation of ethenone ice starts when dust temperatures exceed ~ 100 K. Key removal channels include photodissociation and photoionization, and freeze-out in the disk midplane.

In the presence of dynamical transport, concentrations of HNCO and other COMs are enhanced, albeit differently. This is related to their relatively long chemical time scales associated with slow surface synthesis, which is longer than the dynamical time scales. HCOOH becomes more abundant since concentrations of its precursors, water and HCO^+ , are increased by mixing, leading to higher concentrations of CH_3O^+ . The effect is less pronounced for HNCO, as its precursor species, OCN, is not as sensitive to transport. HNCO ice, produced in the molecular layer, is transported by diffusion to the cold midplane where it cannot be effectively synthesized.

Concentration of gaseous acetaldehyde is greatly enhanced by mixing in the molecular layer at $r \lesssim 100$ AU. It is synthesized via recombination of heavy CH_3 and HCO ices, which are mobile on dust surfaces only in the very inner warm disk region. In the fast mixing model large amounts of solid acetaldehyde accumulate as more and more icy grains reach the warm disk regions due to transport.

To conclude, *in situ* studies of “primitive” material in the solar system have provided mounting evidence for the presence of complex organic matter in the early solar nebula. Complex molecules should also be present in other protoplanetary disks, but only a few key species have been detected so far due to the limited sensitivity of modern (sub)millimeter interferometers. This situation will likely change dramatically with the beginning of the full operation of ALMA. The potential detection of such complex species like dimethyl ether, formic acid, methyl formate, etc. in protoplanetary disks with ALMA will provide solid evidence that the global chemical evolution is regulated by disk dynamics.

7. CONCLUSIONS

Protoplanetary disks are amazing structures of gas and dust surrounding young stars, which are characterized by a broad range in temperature, density, and radiation fields. They show a

rich variety of chemical processes, ranging from high-temperature neutral–neutral reactions in the inner disk regions to ion–molecular chemistry and molecular freeze-out close to the midplane in the outer disk regions. Grain surface reactions, thermal and photodriven desorption, as well as deuteration processes are all part of the diverse chemistry in protoplanetary disks. Dust evolution, ionization structure, and turbulent transport are closely linked processes, defining the thermal and kinematic structure of disks.

Submillimeter and millimeter observations provide constraints on the radial and vertical physical and chemical structure, and are delivering information about molecular abundances in the outer disks. Infrared spectroscopy both from the ground and from space has been providing an inventory of H₂O, OH, CO, CO₂, and simple organic molecules in the warm planet-forming regions of disks. With the enormously increased sensitivity and spatial resolution provided by the Atacama Large Millimeter/Submillimeter Array in Chile, now beginning operations, and the infrared spectroscopic capabilities of the James Webb Space Telescope, to be launched toward the end of this decade, the field of disk chemistry will become ever more rich in data. The development of theoretical modeling tools and the determination of key reaction rates will form the basis for the comprehensive scientific exploitation of these astronomical data.

AUTHOR INFORMATION

Corresponding Author

*E-mail: henning@mpia.de (T.H.); semenov@mpia.de (D.S.).

Notes

The authors declare no competing financial interest.

Biographies



Thomas Henning is a Director at the Max Planck Institute for Astronomy in Heidelberg leading the Planet and Star Formation Department. He is also a professor of astrophysics at the University of Jena and an honorary professor at the University of Heidelberg. Thomas Henning is a member of the German National Academy of Sciences Leopoldina. He is involved in a number of large astronomical instrumentation projects including the MIRI instrument for the James Webb Space Telescope and the interferometric instrument MATISSE for the Very Large Telescope Interferometer in Chile. He is serving on a number of national and international scientific committees and is editor of the popular astronomy journal *Sterne und Weltraum*. His research interests include the physics and chemistry of molecular clouds and protoplanetary disks and

the formation of stars and planetary systems. He is combining observational data and large-scale numerical simulations with laboratory investigations, especially the spectroscopy of large molecules and nanoparticles.



Dmitry Semenov obtained his Master Degree in Astronomy at Saint-Petersburg State University in Saint-Petersburg, Russia. He obtained his Ph.D. in Astrophysics at Friedrich Schiller University in Jena, Germany, in 2005, under the supervision of Professor Thomas Henning. After that, he moved to the Max Planck Institute for Astronomy in Heidelberg, where he works as a staff scientist. He is a leader of a small astrochemistry team at MPIA, observationally and theoretically studying the molecular composition of protoplanetary disks: enigmatic objects that resemble our solar system during the first several million years of evolution.

ACKNOWLEDGMENTS

This research made use of NASA's Astrophysics Data System. D.S. acknowledges support by the Deutsche Forschungsgemeinschaft through SPP 1385: "The first ten million years of the solar system—a planetary materials approach" (SE 1962/1-1 and 1-2).

REFERENCES

- (1) Mayor, M.; Queloz, D. *Nature* **1995**, *378*, 355.
- (2) Udry, S.; Santos, N. C. *Annu. Rev. Astron. Astrophys.* **2007**, *45*, 397.
- (3) Batalha, N. M.; et al. *Astrophys. J., Suppl. Ser.* **2013**, *204*, 24.
- (4) Barclay, T.; et al. *Nature* **2013**, *494*, 452.
- (5) Stevenson, K. B.; Harrington, J.; Nymeyer, S.; Madhusudhan, N.; Seager, S.; Bowman, W. C.; Hardy, R. A.; Deming, D.; Rauscher, E.; Lust, N. B. *Nature* **2010**, *464*, 1161.
- (6) Barman, T. S.; Macintosh, B.; Konopacky, Q. M.; Marois, C. *Astrophys. J.* **2011**, *733*, 65.
- (7) Konopacky, Q. M.; Barman, T. S.; Macintosh, B. A.; Marois, C. *Science* **2013**, *339*, 1398.
- (8) Kretke, K. A.; Lin, D. N. C. *Astrophys. J.* **2012**, *755*, 74.
- (9) Ida, S.; Lin, D. N. C. *Astrophys. J.* **2004**, *616*, 567.
- (10) Mordasini, C.; Alibert, Y.; Benz, W.; Klahr, H.; Henning, T. *Astron. Astrophys.* **2012**, *541*, A97.
- (11) Mordasini, C.; Alibert, Y.; Klahr, H.; Henning, T. *Astron. Astrophys.* **2012**, *547*, A111.
- (12) Williams, J. P.; Cieza, L. A. *Annu. Rev. Astron. Astrophys.* **2011**, *49*, 67.
- (13) Stahler, S. W.; Palla, F. *The Formation of Stars*; Wiley-VCH Verlag GmbH: Weinheim, 2005.
- (14) Hartmann, L. *Accretion Processes in Star Formation*, 2nd ed.; Cambridge University Press: Cambridge, U.K., 2009.
- (15) Strom, K. M.; Strom, S. E.; Edwards, S.; Cabrit, S.; Skrutskie, M. F. *Astron. J.* **1989**, *97*, 1451.

- (16) Beckwith, S. V. W.; Sargent, A. I.; Chini, R. S.; Güsten, R. *Astron. J.* **1990**, *99*, 924.
- (17) Henning, T.; Meeus, G. In *Physical Processes in Circumstellar Disks around Young Stars*; Garcia, P. J. V., Ed.; Chicago University Press: Chicago, 2011; p 114.
- (18) Grady, C. A.; et al. *Astrophys. J.* **2013**, *762*, 48.
- (19) Hughes, A. M.; Wilner, D. J.; Calvet, N.; D'Alessio, P.; Claussen, M. J.; Hogerheijde, M. R. *Astrophys. J.* **2007**, *664*, 536.
- (20) Ratzka, T.; Leinert, C.; Henning, T.; Bouwman, J.; Dullemond, C. P.; Jaffe, W. *Astron. Astrophys.* **2007**, *471*, 173.
- (21) Brown, J. M.; Blake, G. A.; Qi, C.; Dullemond, C. P.; Wilner, D. J.; Williams, J. P. *Astrophys. J.* **2009**, *704*, 496.
- (22) Brown, J. M.; Herczeg, G. J.; Pontoppidan, K. M.; van Dishoeck, E. F. *Astrophys. J.* **2012**, *744*, 116.
- (23) Sicilia-Aguilar, A.; Hartmann, L.; Calvet, N.; Megeath, S. T.; Muñoz, J.; Allen, L.; D'Alessio, P.; Merín, B.; Stauffer, J.; Young, E.; Lada, C. *Astrophys. J.* **2006**, *638*, 897.
- (24) Sicilia-Aguilar, A.; Henning, T.; Juhász, A.; Bouwman, J.; Garmire, G.; Garmire, A. *Astrophys. J.* **2008**, *687*, 1145.
- (25) Furlan, E.; Watson, D. M.; McClure, M. K.; Manoj, P.; Espaillat, C.; D'Alessio, P.; Calvet, N.; Kim, K. H.; Sargent, B. A.; Forrest, W. J.; Hartmann, L. *Astrophys. J.* **2009**, *703*, 1964.
- (26) Merín, B.; et al. *Astrophys. J.* **2010**, *718*, 1200.
- (27) Espaillat, C.; D'Alessio, P.; Hernández, J.; Nagel, E.; Luhman, K. L.; Watson, D. M.; Calvet, N.; Muñoz, J.; McClure, M. *Astrophys. J.* **2010**, *717*, 441.
- (28) Fukagawa, M.; et al. *Astrophys. J. Lett.* **2004**, *605*, L53.
- (29) van der Marel, N.; van Dishoeck, E. F.; Bruderer, S.; Birnstiel, T.; Pinilla, P.; Dullemond, C. P.; van Kempen, T. A.; Schmalzl, M.; Brown, J. M.; Herczeg, G. J.; Mathews, G. S.; Geers, V. *Science* **2013**, *340*, 1199.
- (30) Flock, M.; Dzyurkevich, N.; Klahr, H.; Turner, N.; Henning, T. *Astrophys. J.* **2012**, *744*, 144.
- (31) Boley, A. C.; Hayfield, T.; Mayer, L.; Durisen, R. H. *Icarus* **2010**, *207*, 509.
- (32) van Dishoeck, E. F. *Proc. Natl. Acad. Sci. U.S.A.* **2006**, *103*, 12249.
- (33) Dutrey, A.; Guilloteau, S.; Ho, P. In *Protostars and Planets V*; Reipurth, B., Jewitt, D., Keil, K., Eds.; University of Arizona Press: Tucson, 2007; p 495.
- (34) Bergin, E. A. In *Physical Processes in Circumstellar Disks around Young Stars*; Garcia, P. J. V., Ed.; Chicago University Press: Chicago, 2011; p 55.
- (35) Aikawa, Y.; Momose, M.; Thi, W.-F.; van Zadelhoff, G.-J.; Qi, C.; Blake, G. A.; van Dishoeck, E. F. *Publ. Astron. Soc. Jpn.* **2003**, *55*, 11.
- (36) Piétu, V.; Dutrey, A.; Guilloteau, S. *Astron. Astrophys.* **2007**, *467*, 163.
- (37) Schreyer, K.; Guilloteau, S.; Semenov, D.; Bacmann, A.; Chapillon, E.; Dutrey, A.; Gueth, F.; Henning, T.; Hersant, F.; Launhardt, R.; Pety, J.; Piétu, V. *Astron. Astrophys.* **2008**, *491*, 821.
- (38) Panić, O.; Hogerheijde, M. R. *Astron. Astrophys.* **2009**, *508*, 707.
- (39) Öberg, K. I.; Qi, C.; Fogel, J. K. J.; Bergin, E. A.; Andrews, S. M.; Espaillat, C.; van Kempen, T. A.; Wilner, D. J.; Pascucci, I. *Astrophys. J.* **2010**, *720*, 480.
- (40) Richling, S.; Yorke, H. W. *Astrophys. J.* **2000**, *539*, 258.
- (41) Willacy, K.; Langer, W. D. *Astrophys. J.* **2000**, *544*, 903.
- (42) van Zadelhoff, G.-J.; Aikawa, Y.; Hogerheijde, M. R.; van Dishoeck, E. F. *Astron. Astrophys.* **2003**, *397*, 789.
- (43) Semenov, D.; Wiebe, D.; Henning, T. *Astron. Astrophys.* **2004**, *417*, 93.
- (44) van Dishoeck, E. F.; Jonkheid, B.; van Hemert, M. C. In *Chemical Evolution of the Universe*; Sims, I. R., Williams, D. A., Eds.; Faraday Discussions; Royal Society of Chemistry: Cambridge, U.K., 2006; Vol. 133, p 231.
- (45) Gorti, U.; Dullemond, C. P.; Hollenbach, D. *Astrophys. J.* **2009**, *705*, 1237.
- (46) Visser, R.; van Dishoeck, E. F.; Black, J. H. *Astron. Astrophys.* **2009**, *503*, 323.
- (47) Henning, T.; Semenov, D.; Guilloteau, S.; Dutrey, A.; Hersant, F.; Wakelam, V.; Chapillon, E.; Launhardt, R.; Piétu, V.; Schreyer, K. *Astrophys. J.* **2010**, *714*, 1511.
- (48) Owen, J. E.; Ercolano, B.; Clarke, C. J. *Mon. Not. R. Astron. Soc.* **2011**, *412*, 13.
- (49) Walsh, C.; Nomura, H.; Millar, T. J.; Aikawa, Y. *Astrophys. J.* **2012**, *747*, 114.
- (50) Dutrey, A.; Guilloteau, S.; Guelin, M. *Astron. Astrophys.* **1997**, *317*, L55.
- (51) Qi, C.; Öberg, K. I.; Wilner, D. J. *Astrophys. J.* **2013**, *765*, 34.
- (52) Glassgold, A. E.; Najita, J.; Igea, J. *Astrophys. J.* **1997**, *480*, 344.
- (53) Ilgner, M.; Nelson, R. P. *Astron. Astrophys.* **2006**, *445*, 205.
- (54) Ilgner, M.; Nelson, R. P. *Astron. Astrophys.* **2006**, *445*, 223.
- (55) Ilgner, M.; Nelson, R. P. *Astron. Astrophys.* **2006**, *455*, 731.
- (56) Oberg, K. I.; Qi, C.; Wilner, D. J.; Andrews, S. M. *Astrophys. J.* **2011**, *743*, 152.
- (57) Balbus, S. A.; Hawley, J. F. *Astrophys. J.* **1991**, *376*, 214.
- (58) Gail, H.-P. *Astron. Astrophys.* **2002**, *390*, 253.
- (59) Wehrstedt, M.; Gail, H. *Astron. Astrophys.* **2002**, *385*, 181.
- (60) Boss, A. P. *Astrophys. J.* **2004**, *616*, 1265.
- (61) Ilgner, M.; Henning, T.; Markwick, A. J.; Millar, T. J. *Astron. Astrophys.* **2004**, *415*, 643.
- (62) Willacy, K.; Langer, W.; Allen, M.; Bryden, G. *Astrophys. J.* **2006**, *644*, 1202.
- (63) Aikawa, Y. *Astrophys. J.* **2007**, *656*, L93.
- (64) Turner, N. J.; Sano, T.; Dziourkevitch, N. *Astrophys. J.* **2007**, *659*, 729.
- (65) Tscharnutter, W. M.; Gail, H.-P. *Astron. Astrophys.* **2007**, *463*, 369.
- (66) Hersant, F.; Wakelam, V.; Dutrey, A.; Guilloteau, S.; Herbst, E. *Astron. Astrophys.* **2009**, *493*, L49.
- (67) Heinzeller, D.; Nomura, H.; Walsh, C.; Millar, T. J. *Astrophys. J.* **2011**, *731*, 115.
- (68) Semenov, D.; Wiebe, D. *Astrophys. J.* **2011**, *196*, 25.
- (69) Lynden-Bell, D.; Pringle, J. E. *Mon. Not. R. Astron. Soc.* **1974**, *168*, 603.
- (70) Pringle, J. E. *Ann. Rev. Astron. Astrophys.* **1981**, *19*, 137.
- (71) Akimkin, V.; Zhukovska, S.; Wiebe, D.; Semenov, D.; Pavlyuchenkov, Y.; Vasyunin, A.; Birnstiel, T.; Henning, T. *Astrophys. J.* **2013**, *766*, 8.
- (72) Shakura, N. I.; Sunyaev, R. A. *Astron. Astrophys.* **1973**, *24*, 337.
- (73) Flock, M.; Dzyurkevich, N.; Klahr, H.; Turner, N. J.; Henning, T. *Astrophys. J.* **2011**, *735*, 122.
- (74) Hueso, R.; Guillot, T. *Astron. Astrophys.* **2005**, *442*, 703.
- (75) Kenyon, S. J.; Hartmann, L. *Astrophys. J.* **1987**, *323*, 714.
- (76) Bell, K. R.; Cassen, P. M.; Klahr, H. H.; Henning, T. *Astrophys. J.* **1997**, *486*, 372.
- (77) Balbus, S. A.; Hawley, J. F. *Rev. Mod. Phys.* **1998**, *70*, 1.
- (78) Gammie, C. F. *Astrophys. J.* **1996**, *457*, 355.
- (79) Sano, T.; Miyama, S. M.; Umebayashi, T.; Nakano, T. *Astrophys. J.* **2000**, *543*, 486.
- (80) Dzyurkevich, N.; Turner, N. J.; Henning, T.; Kley, W. *Astrophys. J.* **2013**, *765*, 114.
- (81) Mohanty, S.; Ercolano, B.; Turner, N. J. *Astrophys. J.* **2013**, *764*, 65.
- (82) Pickett, B. K.; Mejía, A. C.; Durisen, R. H.; Cassen, P. M.; Berry, D. K.; Link, R. P. *Astrophys. J.* **2003**, *590*, 1060.
- (83) Boley, A. C.; Mejía, A. C.; Durisen, R. H.; Cai, K.; Pickett, M. K.; D'Alessio, P. *Astrophys. J.* **2006**, *651*, 517.
- (84) Dullemond, C. P.; Hollenbach, D.; Kamp, I.; D'Alessio, P. In *Protostars and Planets V*; Reipurth, B., Jewitt, D., Keil, K., Eds.; University of Arizona Press: Tucson, 2007; p 555.
- (85) Hirose, S.; Turner, N. J. *Astrophys. J.* **2011**, *732*, L30.
- (86) Bertout, C. *Annu. Rev. Astron. Astrophys.* **1989**, *27*, 351.
- (87) Bergin, E.; Calvet, N.; D'Alessio, P.; Herczeg, G. J. *Astrophys. J.* **2003**, *591*, L159.
- (88) Preibisch, T.; Kim, Y.; Favata, F.; Feigelson, E. D.; Flaccomio, E.; Getman, K.; Micela, G.; Sciortino, S.; Stassun, K.; Stelzer, B.; Zinnecker, H. *Astrophys. J.* **2005**, *160*, 401.

- (89) Waters, L. B. F. M.; Waelkens, C. *Ann. Rev. Astron. Astrophys.* **1998**, *36*, 233.
- (90) Güdel, M.; Nazé, Y. *Astron. Astrophys.* **2009**, *17*, 309.
- (91) Bethell, T. J.; Bergin, E. A. *Astrophys. J.* **2011**, *739*, 78.
- (92) D'Alessio, P.; Calvet, N.; Hartmann, L.; Lizano, S.; Cantó, J. *Astrophys. J.* **1999**, *527*, 893.
- (93) Dullemond, C. P.; Dominik, C.; Natta, A. *Astrophys. J.* **2001**, *560*, 957.
- (94) Gail, H.-P. In *Astromineralogy*, 2nd ed.; Henning, T., Ed.; Lecture Notes in Physics; Springer Verlag: Berlin, 2010; Vol. 815, p 61.
- (95) Kamp, I.; Dullemond, C. P. *Astrophys. J.* **2004**, *615*, 991.
- (96) Gorti, U.; Hollenbach, D. *Astrophys. J.* **2004**, *613*, 424.
- (97) Gorti, U.; Hollenbach, D. *Astrophys. J.* **2008**, *683*, 287.
- (98) Vasyunin, A. I.; Wiebe, D. S.; Birnstiel, T.; Zhukovska, S.; Henning, T.; Dullemond, C. P. *Astrophys. J.* **2011**, *727*, 76.
- (99) Jonkheid, B.; Kamp, I.; Augereau, J.-C.; van Dishoeck, E. F. *Astron. Astrophys.* **2006**, *453*, 163.
- (100) Glassgold, A. E.; Najita, J.; Igea, J. *Astrophys. J.* **2004**, *615*, 972.
- (101) Glassgold, A. E.; Galli, D.; Padovani, M. *Astrophys. J.* **2012**, *756*, 157.
- (102) Brauer, F.; Dullemond, C. P.; Henning, T. *Astron. Astrophys.* **2008**, *480*, 859.
- (103) Beckwith, S. V. W.; Henning, T.; Nakagawa, Y. In *Protostars and Planets IV*; Mannings, V., Boss, A. P., Russell, S. S., Eds.; University of Arizona Press: Tucson, 2000; p 533.
- (104) Weidenschilling, S. J.; Cuzzi, J. N. In *Protostars and Planets III*; Levy, E. H., Lunine, J. I., Eds.; University of Arizona Press: Tucson, 1993; p 1031.
- (105) Birnstiel, T.; Dullemond, C. P.; Brauer, F. *Astron. Astrophys.* **2010**, *513*, A79.
- (106) Haghjipour, N.; Boss, A. P. *Astrophys. J.* **2003**, *598*, 1301.
- (107) Johansen, A.; Klahr, H.; Henning, T. *Astron. Astrophys.* **2011**, *529*, A62.
- (108) Meheut, H.; Meliani, Z.; Varniere, P.; Benz, W. *Astron. Astrophys.* **2012**, *545*, A134.
- (109) Safronov, V. S. *Evoliutsiya Doplanechnogo Oblaka i Obrazovanie Zemli i Planet*; Izdatel'stvo "Nauka": Moskva, USSR, 1969.
- (110) Hayashi, C.; Nakazawa, K.; Nakagawa, Y. In *Protostars and Planets II*; Black, D. C., Matthews, M. S., Eds.; University of Arizona Press: Tucson, 1985; p 1100.
- (111) Pollack, J. B.; Hubickyj, O.; Bodenheimer, P.; Lissauer, J. J.; Podolak, M.; Greenzweig, Y. *Icarus* **1996**, *124*, 62.
- (112) Johansen, A.; Oishi, J. S.; Mac Low, M.-M.; Klahr, H.; Henning, T.; Youdin, A. *Nature* **2007**, *448*, 1022.
- (113) Papaloizou, J. C. B.; Nelson, R. P.; Kley, W.; Masset, F. S.; Artymowicz, P. In *Protostars and Planets V*; Reipurth, B., Jewitt, D., Keil, K., Eds.; University of Arizona Press: Tucson, 2007; p 655.
- (114) Boss, A. P. *Science* **1997**, *276*, 1836.
- (115) Carson, J.; et al. *Astrophys. J., Lett.* **2013**, *763*, L32.
- (116) Janson, M.; Bonavita, M.; Klahr, H.; Lafrenière, D. *Astrophys. J.* **2012**, *745*, 4.
- (117) Carmona, A.; van den Ancker, M. E.; Henning, T.; Pavlyuchenkov, Y.; Dullemond, C. P.; Goto, M.; Thi, W. F.; Bouwman, J.; Waters, L. B. F. M. *Astron. Astrophys.* **2008**, *477*, 839.
- (118) Tielens, A. G. G. M.; Tokunaga, A. T.; Geballe, T. R.; Baas, F. *Astrophys. J.* **1991**, *381*, 181.
- (119) van Dishoeck, E. F. *Rate Coefficients in Astrochemistry*; Millar, T., Williams, D., Eds.; ASSL/Kluwer Academic Publishers: Dordrecht, 1988; Vol. 146, p 49.
- (120) Clayton, R. N. *Nature* **2002**, *415*, 860.
- (121) Lyons, J. R.; Boney, E.; Marcus, R. A. *Lunar and Planetary Institute Conference Abstracts*; Lunar and Planetary Institute Technical Report; Lunar and Planetary Institute: Houston, 2007; Vol. 38, p 2382.
- (122) Schreyer, K.; Semenov, D.; Henning, T.; Forbrich, J. *Astrophys. J.* **2006**, *637*, L129.
- (123) Bergin, E. A.; Cleeves, L. I.; Gorti, U.; Zhang, K.; Blake, G. A.; Green, J. D.; Andrews, S. M.; Evans, N. J., II; Henning, T.; Öberg, K.; Pontoppidan, K.; Qi, C.; Salyk, C.; van Dishoeck, E. *Nature* **2013**, *493*, 644.
- (124) Andrews, S. M.; Williams, J. P. *Astrophys. J.* **2005**, *631*, 1134.
- (125) Andrews, S. M.; Williams, J. P. *Astrophys. J.* **2007**, *671*, 1800.
- (126) Guilloteau, S.; Dutrey, A.; Piétu, V.; Boehler, Y. *Astron. Astrophys.* **2011**, *529*, A105.
- (127) Andrews, S. M.; Rosenfeld, K. A.; Kraus, A. L.; Wilner, D. J. *Astrophys. J.* **2013**, *771*, 129.
- (128) Muzerolle, J.; Hillenbrand, L.; Calvet, N.; Briceño, C.; Hartmann, L. *Astrophys. J.* **2003**, *592*, 266.
- (129) Natta, A.; Testi, L.; Randich, S. *Astron. Astrophys.* **2006**, *452*, 245.
- (130) Fang, M.; van Boekel, R.; Wang, W.; Carmona, A.; Sicilia-Aguilar, A.; Henning, T. *Astron. Astrophys.* **2009**, *504*, 461.
- (131) Fedele, D.; van den Ancker, M. E.; Henning, T.; Jayawardhana, R.; Oliveira, J. M. *Astron. Astrophys.* **2010**, *510*, A72.
- (132) Andrews, S. M.; Wilner, D. J.; Hughes, A. M.; Qi, C.; Rosenfeld, K. A.; Öberg, K. I.; Birnstiel, T.; Espaillat, C.; Cieza, L. A.; Williams, J. P.; Lin, S.-Y.; Ho, P. T. P. *Astrophys. J.* **2012**, *744*, 162.
- (133) Guilloteau, S.; Dutrey, A. *Astron. Astrophys.* **1998**, *339*, 467.
- (134) Panić, O.; Hogerheijde, M. R.; Wilner, D.; Qi, C. *Astron. Astrophys.* **2008**, *491*, 219.
- (135) Qi, C.; Wilner, D. J.; Calvet, N.; Bourke, T. L.; Blake, G. A.; Hogerheijde, M. R.; Ho, P. T. P.; Bergin, E. *Astrophys. J.* **2006**, *636*, L157.
- (136) Akiyama, E.; Momose, M.; Hayashi, H.; Kitamura, Y. arXiv:astro-ph/1205.6573, 2012.
- (137) Dartois, E.; Dutrey, A.; Guilloteau, S. *Astron. Astrophys.* **2003**, *399*, 773.
- (138) Haisch, K. E.; Lada, E. A.; Lada, C. J. *Astrophys. J.* **2001**, *553*, L153.
- (139) Moór, A.; Ábrahám, P.; Juhász, A.; Kiss, C.; Pascucci, I.; Kóspál, Á.; Apai, D.; Henning, T.; Csengeri, T.; Grady, C. *Astrophys. J.* **2011**, *740*, L7.
- (140) Amelin, Y.; Krot, A. *Meteorit. Planet. Sci.* **2007**, *42*, 1321.
- (141) Dutrey, A.; Henning, T.; Guilloteau, S.; Semenov, D.; Piétu, V.; Schreyer, K.; Bacmann, A.; Launhardt, R.; Pety, J.; Gueth, F. *Astron. Astrophys.* **2007**, *464*, 615.
- (142) Dutrey, A.; Wakelam, V.; Boehler, Y.; Guilloteau, S.; Hersant, F.; Semenov, D.; Chapillon, E.; Henning, T.; Piétu, V.; Launhardt, R.; Gueth, F.; Schreyer, K. *Astron. Astrophys.* **2011**, *535*, A104.
- (143) Chapillon, E.; Guilloteau, S.; Dutrey, A.; Piétu, V.; Guélin, M. *Astron. Astrophys.* **2012**, *537*, A60.
- (144) Chapillon, E.; Dutrey, A.; Guilloteau, S.; Piétu, V.; Wakelam, V.; Hersant, F.; Gueth, F.; Henning, T.; Launhardt, R.; Schreyer, K.; Semenov, D. *Astrophys. J.* **2012**, *756*, 58.
- (145) Guilloteau, S.; Dutrey, A.; Wakelam, V.; Hersant, F.; Semenov, D.; Chapillon, E.; Henning, T.; Piétu, V. *Astron. Astrophys.* **2012**, *548*, A70.
- (146) Öberg, K. I.; Qi, C.; Fogel, J. K. J.; Bergin, E. A.; Andrews, S. M.; Espaillat, C.; Wilner, D. J.; Pascucci, I.; Kastner, J. H. *Astrophys. J.* **2011**, *734*, 98.
- (147) Qi, C.; Öberg, K. I.; Wilner, D. J.; Rosenfeld, K. A. *Astrophys. J., Lett.* **2013**, *765*, L14.
- (148) Kastner, J. H.; Zuckerman, B.; Weintraub, D. A.; Forveille, T. *Science* **1997**, *277*, 67.
- (149) Fedele, D.; Bruderer, S.; van Dishoeck, E. F.; Herczeg, G. J.; Evans, N. J.; Bouwman, J.; Henning, T.; Green, J. *Astron. Astrophys.* **2012**, *544*, L9.
- (150) Meeus, G.; et al. *Astron. Astrophys.* **2012**, *544*, A78.
- (151) Riviere-Marichalar, P.; Ménard, F.; Thi, W. F.; Kamp, I.; Montesinos, B.; Meeus, G.; Woitke, P.; Howard, C.; Sandell, G.; Podio, L.; Dent, W. R. F.; Mendigutía, I.; Pinte, C.; White, G. J.; Barrado, D. *Astron. Astrophys.* **2012**, *538*, L3.
- (152) Fedele, D.; Bruderer, S.; van Dishoeck, E. F.; Carr, J.; Herczeg, G. J.; Salyk, C.; Evans, N. J., II; Bouwman, J.; Meeus, G.; Henning, T.; Green, J.; Najita, J. R.; Guedel, M. ArXiv:astro-ph/1308.1578, 2013
- (153) Hogerheijde, M. R.; Bergin, E. A.; Brinch, C.; Cleeves, L. I.; Fogel, J. K. J.; Blake, G. A.; Dominik, C.; Lis, D. C.; Melnick, G.;

- Neufeld, D.; Panić, O.; Pearson, J. C.; Kristensen, L.; Yldz, U. A.; van Dishoeck, E. F. *Science* **2011**, *334*, 338.
- (154) Sturm, B.; et al. *Astron. Astrophys.* **2010**, *518*, L129.
- (155) Meeus, G.; Salyk, C.; Bruderer, S.; Fedele, D.; Maaskant, K.; Evans, N. J., II; van Dishoeck, E. F.; Montesinos, B.; Herczeg, G.; Bouwman, J.; Green, J. D.; Dominik, C.; Henning, T.; Vicente, S. The DIGIT Team, ArXiv:astro-ph/1308.4160, 2013.
- (156) Bruderer, S.; van Dishoeck, E. F.; Doty, S. D.; Herczeg, G. J. *Astron. Astrophys.* **2012**, *541*, A91.
- (157) Thi, W.-F.; et al. *Astron. Astrophys.* **2011**, *530*, L2.
- (158) Carr, J. S.; Najita, J. R. *Science* **2008**, *319*, 1504.
- (159) Salyk, C.; Pontoppidan, K. M.; Blake, G. A.; Lahuis, F.; van Dishoeck, E. F.; Evans, N. J., II. *Astrophys. J.* **2008**, *676*, L49.
- (160) Pascucci, I.; Apai, D.; Luhman, K.; Henning, T.; Bouwman, J.; Meyer, M. R.; Lahuis, F.; Natta, A. *Astrophys. J.* **2009**, *696*, 143.
- (161) Pontoppidan, K. M.; Salyk, C.; Blake, G. A.; Käufl, H. U. *Astrophys. J.* **2010**, *722*, L173.
- (162) Carr, J. S.; Najita, J. R. *Astrophys. J.* **2011**, *733*, 102.
- (163) Salyk, C.; Pontoppidan, K. M.; Blake, G. A.; Najita, J. R.; Carr, J. S. *Astrophys. J.* **2011**, *731*, 130.
- (164) Mandell, A. M.; Bast, J.; van Dishoeck, E. F.; Blake, G. A.; Salyk, C.; Mumma, M. J.; Villanueva, G. *Astrophys. J.* **2012**, *747*, 92.
- (165) Lahuis, F.; van Dishoeck, E. F.; Boogert, A. C. A.; Pontoppidan, K. M.; Blake, G. A.; Dullemond, C. P.; Evans, N. J., II; Hogerheijde, M. R.; Jørgensen, J. K.; Kessler-Silacci, J. E.; Knez, C. *Astrophys. J.* **2006**, *636*, L145.
- (166) Gibb, E. L.; Van Brunt, K. A.; Brittain, S. D.; Rettig, T. W. *Astrophys. J.* **2007**, *660*, 1572.
- (167) Pontoppidan, K. M.; Salyk, C.; Blake, G. A.; Meijerink, R.; Carr, J. S.; Najita, J. *Astrophys. J.* **2010**, *720*, 887.
- (168) Brittain, S. D.; Rettig, T. W.; Simon, T.; Kulesa, C.; DiSanti, M. A.; Dello Russo, N. *Astrophys. J.* **2003**, *588*, 535.
- (169) Pontoppidan, K. M.; Blake, G. A.; van Dishoeck, E. F.; Smette, A.; Ireland, M. J.; Brown, J. *Astrophys. J.* **2008**, *684*, 1323.
- (170) Najita, J.; Carr, J. S.; Mathieu, R. D. *Astrophys. J.* **2003**, *589*, 931.
- (171) Najita, J. R.; Carr, J. S.; Glassgold, A. E.; Valenti, J. A. In *Protostars and Planets V*; Reipurth, B., Jewitt, D., Keil, K., Eds.; University of Arizona Press: Tucson, 2007; p 507.
- (172) Thrower, J. D.; Jørgensen, B.; Friis, E. E.; Baouche, S.; Mennella, V.; Luntz, A. C.; Andersen, M.; Hammer, B.; Hornekær, L. *Astrophys. J.* **2012**, *752*, 3.
- (173) Acke, B.; Bouwman, J.; Juhász, A.; Henning, T.; van den Ancker, M. E.; Meeus, G.; Tielens, A. G. G. M.; Waters, L. B. F. M. *Astrophys. J.* **2010**, *718*, 558.
- (174) Geers, V. C.; van Dishoeck, E. F.; Visser, R.; Pontoppidan, K. M.; Augereau, J.-C.; Habart, E.; Lagrange, A. M. *Astron. Astrophys.* **2007**, *476*, 279.
- (175) Siebenmorgen, R.; Krügel, E. *Astron. Astrophys.* **2010**, *511*, A6.
- (176) Tiné, S.; Roueff, E.; Falgarone, E.; Gerin, M.; Pineau des Forets, G. *Astron. Astrophys.* **2000**, *356*, 1039.
- (177) Roberts, H.; Fuller, G. A.; Millar, T. J.; Hatchell, J.; Buckle, J. V. *Astron. Astrophys.* **2002**, *381*, 1026.
- (178) Guilloteau, S.; Piétu, V.; Dutrey, A.; Guélin, M. *Astron. Astrophys.* **2006**, *448*, L5.
- (179) Caselli, P.; Vastel, C.; Ceccarelli, C.; van der Tak, F. F. S.; Crapsi, A.; Bacmann, A. *Astron. Astrophys.* **2008**, *492*, 703.
- (180) Chapillon, E.; Parise, B.; Guilloteau, S.; Du, F. *Astron. Astrophys.* **2011**, *533*, 143.
- (181) Öberg, K. I.; Qi, C.; Wilner, D. J.; Hogerheijde, M. R. *Astrophys. J.* **2012**, *749*, 162.
- (182) Natta, A.; Testi, L.; Calvet, N.; Henning, T.; Waters, R.; Wilner, D. In *Protostars and Planets V*; Reipurth, B., Jewitt, D., Keil, K., Eds.; University of Arizona Press: Tucson, 2007; p 767.
- (183) Juhász, A.; Bouwman, J.; Henning, T.; Acke, B.; van den Ancker, M. E.; Meeus, G.; Dominik, C.; Min, M.; Tielens, A. G. G. M.; Waters, L. B. F. M. *Astrophys. J.* **2010**, *721*, 431.
- (184) van Boekel, R.; Min, M.; Waters, L. B. F. M.; de Koter, A.; Dominik, C.; van den Ancker, M. E.; Bouwman, J. *Astron. Astrophys.* **2005**, *437*, 189.
- (185) Bouwman, J.; Henning, T.; Hillenbrand, L. A.; Meyer, M. R.; Pascucci, I.; Carpenter, J.; Hines, D.; Kim, J. S.; Silverstone, M. D.; Hollenbach, D.; Wolf, S. *Astrophys. J.* **2008**, *683*, 479.
- (186) Meeus, G.; Juhász, A.; Henning, T.; Bouwman, J.; Chen, C.; Lawson, W.; Apai, D.; Pascucci, I.; Sicilia-Aguilar, A. *Astron. Astrophys.* **2009**, *497*, 379.
- (187) Testi, L.; Natta, A.; Shepherd, D. S.; Wilner, D. J. *Astron. Astrophys.* **2003**, *403*, 323.
- (188) Wilner, D. J.; D'Alessio, P.; Calvet, N.; Claussen, M. J.; Hartmann, L. *Astrophys. J. Lett.* **2005**, *626*, L109.
- (189) Rodmann, J.; Henning, T.; Chandler, C. J.; Mundy, L. G.; Wilner, D. J. *Astron. Astrophys.* **2006**, *446*, 211.
- (190) Pérez, L. M.; et al. *Astrophys. J. Lett.* **2012**, *760*, L17.
- (191) Sturm, B.; et al. *Astron. Astrophys.* **2013**, *553*, A5.
- (192) Gail, H.-P. *Astron. Astrophys.* **2004**, *413*, 571.
- (193) Harker, D. E.; Desch, S. J. *Astrophys. J.* **2002**, *565*, L109.
- (194) Ábrahám, P.; Juhász, A.; Dullemond, C. P.; Kóspál, Á.; van Boekel, R.; Bouwman, J.; Henning, T.; Moór, A.; Mosoni, L.; Sicilia-Aguilar, A.; Sipos, N. *Nature* **2009**, *459*, 224.
- (195) Juhász, A.; Dullemond, C. P.; van Boekel, R.; Bouwman, J.; Ábrahám, P.; Acosta-Pulido, J. A.; Henning, T.; Kóspál, Á.; Sicilia-Aguilar, A.; Jones, A.; Moór, A.; Mosoni, L.; Regály, Z.; Szokoly, G.; Sipos, N. *Astrophys. J.* **2012**, *744*, 118.
- (196) Pollack, J. B.; Hollenbach, D.; Beckwith, S.; Simonelli, D. P.; Roush, T.; Fong, W. *Astrophys. J.* **1994**, *421*, 615.
- (197) Semenov, D.; Henning, T.; Helling, C.; Ilgner, M.; Sedlmayr, E. *Astron. Astrophys.* **2003**, *410*, 611.
- (198) Acke, B.; van den Ancker, M. E. *Astron. Astrophys.* **2006**, *457*, 171.
- (199) Guillot, O.; Ledoux, G.; Reynaud, C. *Astrophys. J.* **1999**, *521*, L133.
- (200) Terada, H.; Tokunaga, A. T.; Kobayashi, N.; Takato, N.; Hayano, Y.; Takami, H. *Astrophys. J.* **2007**, *667*, 303.
- (201) Aikawa, Y.; Kamuro, D.; Sakon, I.; Itoh, Y.; Terada, H.; Noble, J. A.; Pontoppidan, K. M.; Fraser, H. J.; Tamura, M.; Kandori, R.; Kawamura, A.; Ueno, M. *Astron. Astrophys.* **2012**, *538*, A57.
- (202) Thi, W. F.; Pontoppidan, K. M.; van Dishoeck, E. F.; Dartois, E.; d'Hendecourt, L. *Astron. Astrophys.* **2002**, *394*, L27.
- (203) Pontoppidan, K. M.; Dullemond, C. P.; van Dishoeck, E. F.; Blake, G. A.; Boogert, A. C. A.; Evans, N. J., II; Kessler-Silacci, J. E.; Lahuis, F. *Astrophys. J.* **2005**, *622*, 463.
- (204) Malfait, K.; Waelkens, C.; Bouwman, J.; de Koter, A.; Waters, L. B. F. M. *Astron. Astrophys.* **1999**, *345*, 181.
- (205) McClure, M. K.; Manoj, P.; Calvet, N.; Adame, L.; Espaillat, C.; Watson, D. M.; Sargent, B.; Forrest, W. J.; D'Alessio, P. *Astrophys. J. Lett.* **2012**, *759*, 10.
- (206) Harada, N.; Herbst, E.; Wakelam, V. *Astrophys. J.* **2010**, *721*, 1570.
- (207) Aikawa, Y.; Umebayashi, T.; Nakano, T.; Miyama, S. M. *Astrophys. J.* **1999**, *519*, 705.
- (208) Willacy, K.; Klahr, H. H.; Millar, T. J.; Henning, T. *Astron. Astrophys.* **1998**, *338*, 995.
- (209) Markwick, A. J.; Ilgner, M.; Millar, T. J.; Henning, T. *Astron. Astrophys.* **2002**, *385*, 632.
- (210) Woods, P. M.; Willacy, K. *Astrophys. J.* **2007**, *655*, L49.
- (211) Bethell, T.; Bergin, E. *Science* **2009**, *326*, 1675.
- (212) Najita, J. R.; Adámkovics, M.; Glassgold, A. E. *Astrophys. J.* **2011**, *743*, 147.
- (213) Fedele, D.; Pascucci, I.; Brittain, S.; Kamp, I.; Woitke, P.; Williams, J. P.; Dent, W. R. F.; Thi, W.-F. *Astrophys. J.* **2011**, *732*, 106.
- (214) Aikawa, Y.; Herbst, E. *Astron. Astrophys.* **1999**, *351*, 233.
- (215) Aikawa, Y.; van Zadelhoff, G. J.; van Dishoeck, E. F.; Herbst, E. *Astron. Astrophys.* **2002**, *386*, 622.
- (216) Fogel, J. K. J.; Bethell, T. J.; Bergin, E. A.; Calvet, N.; Semenov, D. *Astrophys. J.* **2011**, *726*, 29.
- (217) Herbst, E.; Klemperer, W. *Astrophys. J.* **1973**, *185*, 505.

- (218) Watson, W. D. *Astrophys. J.* **1974**, *188*, 35.
- (219) Woodall, J.; Agúndez, M.; Markwick-Kemper, A. J.; Millar, T. J. *Astron. Astrophys.* **2007**, *466*, 1197.
- (220) Wakelam, V.; et al. *Astrophys. J., Suppl. Ser.* **2012**, *199*, 21.
- (221) Morbidelli, A.; Chambers, J.; Lunine, J. I.; Petit, J. M.; Robert, F.; Valsecchi, G. B.; Cyr, K. E. *Meteorit. Planet. Sci.* **2000**, *35*, 1309.
- (222) Lecar, M.; Podolak, M.; Sasselov, D.; Chiang, E. *Astrophys. J.* **2006**, *640*, 1115.
- (223) Encrenaz, T. *Annu. Rev. Astron. Astrophys.* **2008**, *46*, 57.
- (224) Min, M.; Dullemond, C. P.; Kama, M.; Dominik, C. *Icarus* **2011**, *212*, 416.
- (225) Zhang, K.; Pontoppidan, K. M.; Salyk, C.; Blake, G. A. *Astrophys. J.* **2013**, *766*, 82.
- (226) Herczeg, G. J.; Linsky, J. L.; Valenti, J. A.; Johns-Krull, C. M.; Wood, B. E. *Astrophys. J.* **2002**, *572*, 310.
- (227) Schindhelm, E.; France, K.; Herczeg, G. J.; Bergin, E.; Yang, H.; Brown, A.; Brown, J. M.; Linsky, J. L.; Valenti, J. *Astrophys. J., Lett.* **2012**, *756*, L23.
- (228) Semenov, D.; Pavlyuchenkov, Y.; Schreyer, K.; Henning, T.; Dullemond, C.; Bacmann, A. *Astrophys. J.* **2005**, *621*, 853.
- (229) Draine, B. T. *Astrophys. J.* **1978**, *36*, 595.
- (230) van Dishoeck, E. F.; Black, J. H. *Astrophys. J.* **1988**, *334*, 771.
- (231) Draine, B. T.; Bertoldi, F. *Astrophys. J.* **1996**, *468*, 269.
- (232) Getman, K. V.; Feigelson, E. D.; Luhman, K. L.; Sicilia-Aguilar, A.; Wang, J.; Garmire, G. P. *Astrophys. J.* **2009**, *699*, 1454.
- (233) Öberg, K. I.; Fuchs, G. W.; Awad, Z.; Fraser, H. J.; Schlemmer, S.; van Dishoeck, E. F.; Linnartz, H. *Astrophys. J.* **2007**, *662*, L23.
- (234) Öberg, K. I.; van Dishoeck, E. F.; Linnartz, H. *Astron. Astrophys.* **2009**, *496*, 281.
- (235) Öberg, K. I.; Linnartz, H.; Visser, R.; van Dishoeck, E. F. *Astrophys. J.* **2009**, *693*, 1209.
- (236) Fayolle, E. C.; Bertin, M.; Romanzin, C.; Michaut, X.; Öberg, K. I.; Linnartz, H.; Fillion, J.-H. *Astrophys. J.* **2011**, *739*, L36.
- (237) Leger, A.; Jura, M.; Omont, A. *Astron. Astrophys.* **1985**, *144*, 147.
- (238) Hasegawa, T. I.; Herbst, E. *Mon. Not. R. Astron. Soc.* **1993**, *263*, 589.
- (239) Najita, J.; Bergin, E. A.; Ullom, J. N. *Astrophys. J.* **2001**, *561*, 880.
- (240) Cameron, A. G. W. *Meteoritics* **1995**, *30*, 133.
- (241) Grossman, L. *Geochim. Cosmochim. Acta* **1972**, *36*, 597.
- (242) Morfill, G. E.; Völk, H. J. *Astrophys. J.* **1984**, *287*, 371.
- (243) Wood, J. A.; Hashimoto, A. *Geochim. Cosmochim. Acta* **1993**, *57*, 2377.
- (244) Prinn, R. G. In *Protostars and Planets III*; Levy, E. H., Lunine, J. I., Eds.; University of Arizona Press: Tucson, 1993; p 1005.
- (245) Duschl, W. J.; Gail, H.; Tscharnutter, W. M. *Astron. Astrophys.* **1996**, *312*, 624.
- (246) Bauer, I.; Finocchi, F.; Duschl, W. J.; Gail, H.-P.; Schloeder, J. P. *Astron. Astrophys.* **1997**, *317*, 273.
- (247) Finocchi, F.; Gail, H.-P.; Duschl, W. J. *Astron. Astrophys.* **1997**, *325*, 1264.
- (248) Finocchi, F.; Gail, H.-P. *Astron. Astrophys.* **1997**, *327*, 825.
- (249) Gail, H.-P. *Astron. Astrophys.* **1998**, *332*, 1099.
- (250) Gail, H.-P. *Astron. Astrophys.* **2001**, *378*, 192.
- (251) Keller, C.; Gail, H. *Astron. Astrophys.* **2004**, *415*, 1177.
- (252) Lyons, J. R.; Young, E. D. *Nature* **2005**, *435*, 317.
- (253) Ciesla, F. J.; Cuzzi, J. N. *Icarus* **2006**, *181*, 178.
- (254) Ciesla, F. J. *Icarus* **2009**, *200*, 655.
- (255) Geiss, J.; Reeves, H. *Astron. Astrophys.* **1981**, *93*, 189.
- (256) Petaev, M. I.; Wood, J. A. *Meteorit. Planet. Sci.* **1998**, *33*, 1123.
- (257) Fegley, B., Jr. *Space Sci. Rev.* **2000**, *92*, 177.
- (258) Aikawa, Y.; Miyama, S. M.; Nakano, T.; Umebayashi, T. *Astrophys. J.* **1996**, *467*, 684.
- (259) Aikawa, Y.; Umebayashi, T.; Nakano, T.; Miyama, S. M. *Astrophys. J., Lett.* **1997**, *486*, L51.
- (260) Aikawa, Y.; Nomura, H. *Astrophys. J.* **2006**, *642*, 1152.
- (261) Agúndez, M.; Cernicharo, J.; Goicoechea, J. R. *Astron. Astrophys.* **2008**, *483*, 831.
- (262) Walsh, C.; Millar, T. J.; Nomura, H. *Astrophys. J.* **2010**, *722*, 1607.
- (263) D'Alessio, P.; Canto, J.; Calvet, N.; Lizano, S. *Astrophys. J.* **1998**, *500*, 411.
- (264) Weingartner, J. C.; Draine, B. T. *Astrophys. J.* **2001**, *548*, 296.
- (265) Woitke, P.; Kamp, I.; Thi, W. *Astron. Astrophys.* **2009**, *501*, 383.
- (266) Nomura, H.; Aikawa, Y.; Tsujimoto, M.; Nakagawa, Y.; Millar, T. J. *Astrophys. J.* **2007**, *661*, 334.
- (267) Glassgold, A. E.; Feigelson, E. D.; Montmerle, T.; Wolk, S. In *Chondrites and the Protoplanetary Disk*; Krot, A. N., Scott, E. R. D., Reipurth, B., Eds.; Astronomical Society of the Pacific Conference Series; Astronomical Society of the Pacific: San Francisco, 2005; Vol. 341; p 165.
- (268) Aresu, G.; Kamp, I.; Meijerink, R.; Woitke, P.; Thi, W.; Spaans, M. *Astron. Astrophys.* **2011**, *526*, 163.
- (269) Aikawa, Y.; Herbst, E. *Astrophys. J.* **1999**, *526*, 314.
- (270) Aikawa, Y.; Herbst, E. *Astron. Astrophys.* **2001**, *371*, 1107.
- (271) Ceccarelli, C.; Dominik, C. *Astron. Astrophys.* **2005**, *440*, 583.
- (272) Willacy, K. *Astrophys. J.* **2007**, *660*, 441.
- (273) Willacy, K.; Woods, P. M. *Astrophys. J.* **2009**, *703*, 479.
- (274) Woods, P. M.; Willacy, K. *Astrophys. J.* **2009**, *693*, 1360.
- (275) Nomura, H.; Aikawa, Y.; Nakagawa, Y.; Millar, T. J. *Astron. Astrophys.* **2009**, *495*, 183.
- (276) Visser, R.; Doty, S. D.; van Dishoeck, E. F. *Astron. Astrophys.* **2011**, *534*, 132.
- (277) Ilgner, M.; Nelson, R. P. *Astron. Astrophys.* **2008**, *483*, 815.
- (278) Semenov, D.; Wiebe, D.; Henning, T. *Astrophys. J.* **2006**, *647*, L57.
- (279) Turner, N. J.; Willacy, K.; Bryden, G.; Yorke, H. W. *Astrophys. J.* **2006**, *639*, 1218.
- (280) Vorobyov, E. I.; Basu, S. *Astrophys. J.* **2006**, *650*, 956.
- (281) Vorobyov, E. I.; Basu, S. *Astrophys. J.* **2010**, *719*, 1896.
- (282) Ilee, J. D.; Boley, A. C.; Caselli, P.; Durisen, R. H.; Hartquist, T. W.; Rawlings, J. M. C. *Mon. Not. R. Astron. Soc.* **2011**, *417*, 2950.
- (283) Pavlyuchenkov, Y.; Semenov, D.; Henning, T.; Guilloteau, S.; Piétu, V.; Launhardt, R.; Dutrey, A. *Astrophys. J.* **2007**, *669*, 1262.
- (284) Semenov, D.; Pavlyuchenkov, Y.; Henning, T.; Wolf, S.; Launhardt, R. *Astrophys. J., Lett.* **2008**, *673*, L195.
- (285) Kamp, I.; Woitke, P.; Pinte, C.; Tilling, I.; Thi, W.-F.; Menard, F.; Duchene, G.; Augereau, J.-C. *Astron. Astrophys.* **2011**, *532*, A85.
- (286) Igea, J.; Glassgold, A. E. *Astrophys. J.* **1999**, *518*, 848.
- (287) Pierce, D. M.; A'Hearn, M. F. *Astrophys. J.* **2010**, *718*, 340.
- (288) Hayashi, C. *Prog. Theor. Phys. Suppl.* **1981**, *70*, 35.
- (289) Aikawa, Y.; Umebayashi, T.; Nakano, T.; Miyama, S. *Faraday Discussions*; Royal Society of Chemistry: Cambridge, U.K., 1998; Vol. 109, p 281.
- (290) Chiang, E. I.; Goldreich, P. *Astrophys. J.* **1997**, *490*, 368.
- (291) Kamp, I.; van Zadelhoff, G.-J. *Astron. Astrophys.* **2001**, *373*, 641.
- (292) Kamp, I.; Bertoldi, F. *Astron. Astrophys.* **2000**, *353*, 276.
- (293) Millar, T. J.; Nomura, H.; Markwick, A. J. *Astrophys. Space Sci.* **2003**, *285*, 761.
- (294) Glassgold, A. E.; Najita, J. R.; Igea, J. *Astrophys. J.* **2007**, *656*, 515.
- (295) Meijerink, R.; Glassgold, A. E.; Najita, J. R. *Astrophys. J.* **2008**, *676*, 518.
- (296) Glassgold, A. E.; Meijerink, R.; Najita, J. R. *Astrophys. J.* **2009**, *701*, 142x.
- (297) Jonkheid, B.; Faas, F. G. A.; van Zadelhoff, G.-J.; van Dishoeck, E. F. *Astron. Astrophys.* **2004**, *428*, 511.
- (298) Dullemond, C. P.; van Zadelhoff, G. J.; Natta, A. *Astron. Astrophys.* **2002**, *389*, 464.
- (299) Dominik, C.; Ceccarelli, C.; Hollenbach, D.; Kaufman, M. *Astrophys. J.* **2005**, *635*, L85.
- (300) Dullemond, C. P.; Dominik, C. *Astron. Astrophys.* **2004**, *417*, 159.
- (301) Nomura, H.; Millar, T. J. *Astron. Astrophys.* **2005**, *438*, 923.
- (302) Mathis, J. S.; Rumpl, W.; Nordsieck, K. H. *Astrophys. J.* **1977**, *217*, 425.

- (303) Semenov, D.; Hersant, F.; Wakelam, V.; Dutrey, A.; Chapillon, E.; Guilloteau, S.; Henning, T.; Launhardt, R.; Piétu, V.; Schreyer, K. *Astron. Astrophys.* **2010**, *522*, A42.
- (304) Jonkheid, B.; Dullemond, C. P.; Hogerheijde, M. R.; van Dishoeck, E. F. *Astron. Astrophys.* **2007**, *463*, 203.
- (305) Oppenheimer, M.; Dalgarno, A. *Astrophys. J.* **1974**, *192*, 29.
- (306) D'Alessio, P.; Calvet, N.; Hartmann, L. *Astrophys. J.* **2001**, *553*, 321.
- (307) Chapillon, E.; Guilloteau, S.; Dutrey, A.; Piétu, V. *Astron. Astrophys.* **2008**, *488*, 565.
- (308) Chapillon, E.; Parise, B.; Guilloteau, S.; Dutrey, A.; Wakelam, V. *Astron. Astrophys.* **2010**, *520*, 61.
- (309) Vasyunin, A. I.; Semenov, D.; Henning, T.; Wakelam, V.; Herbst, E.; Sobolev, A. M. *Astrophys. J.* **2008**, *672*, 629.
- (310) Visser, R.; van Dishoeck, E. F.; Doty, S. D.; Dullemond, C. P. *Astron. Astrophys.* **2009**, *495*, 881.
- (311) Woitke, P.; et al. *Astron. Astrophys.* **2011**, *534*, 44.
- (312) Meijerink, R.; Aresu, G.; Kamp, I.; Spaans, M.; Thi, W.-F.; Woitke, P. *Astron. Astrophys.* **2012**, *547*, A68.
- (313) Pinte, C.; Ménard, F.; Duchêne, G.; Bastien, P. *Astron. Astrophys.* **2006**, *459*, 797.
- (314) Cleeves, L. I.; Bergin, E. A.; Bethell, T. J.; Calvet, N.; Fogel, J. K. J.; Sauter, J.; Wolf, S. *Astrophys. J., Lett.* **2011**, *743*, L2.
- (315) Bjorkman, J. E.; Wood, K. *Astrophys. J.* **2001**, *554*, 615.
- (316) Bruderer, S.; Benz, A. O.; Doty, S. D.; van Dishoeck, E. F.; Bourke, T. L. *Astrophys. J.* **2009**, *700*, 872.
- (317) Birnstiel, T.; Klahr, H.; Ercolano, B. *Astron. Astrophys.* **2012**, *539*, 148.
- (318) Yurimoto, H.; Kuramoto, K.; Krot, A. N.; Scott, E. R. D.; Cuzzi, J. N.; Thiemens, M. H.; Lyons, J. R. In *Protostars and Planets V*; Reipurth, B., Jewitt, D., Keil, K., Eds.; University of Arizona Press: Tucson, 2007; p 849.
- (319) Draine, B. T. *Annu. Rev. Astron. Astrophys.* **2003**, *41*, 241.
- (320) Palme, H. *Philos. Trans. R. Soc., A* **2001**, *359*, 2061.
- (321) Trieloff, M.; Palme, H. In *Planet Formation*; Klahr, H., Brandner, W., Eds.; Cambridge University Press: Cambridge, U.K., 2006; p 64.
- (322) Ehrenfreund, P.; Charnley, S. B. *Annu. Rev. Astron. Astrophys.* **2000**, *38*, 427.
- (323) Busemann, H.; Young, A. F.; Alexander, C. M.O'D.; Hoppe, P.; Mukhopadhyay, S.; Nittler, L. R. *Science* **2006**, *312*, 727.
- (324) Pizzarello, S.; Cooper, G. W.; Flynn, G. J. In *Meteorites and the Early Solar System II*; Lauretta, D. S., McSween, H. Y., Eds.; University of Arizona Press: Tucson, 2006; p 625.
- (325) Herbst, E.; van Dishoeck, E. F. *Annu. Rev. Astron. Astrophys.* **2009**, *47*, 427.
- (326) Morgan, W. A., Jr.; Feigelson, E. D.; Wang, H.; Frenklach, M. *Science* **1991**, *252*, 109.
- (327) Wozniakiewicz, P. J.; Kearsley, A. T.; Ishii, H. A.; Burchell, M. J.; Bradley, J. P.; Teslich, N.; Cole, M. J.; Price, M. C. *Meteorit. Planet. Sci.* **2012**, *47*, 660.
- (328) Crovisier, J.; Leech, K.; Bockelée-Morvan, D.; Brooke, T. Y.; Hanner, M. S.; Altieri, B.; Keller, H. U.; Lellouch, E. *Science* **1997**, *275*, 1904.
- (329) Kelley, M. S.; Woodward, C. E.; Harker, D. E.; Wooden, D. H.; Gehrz, R. D.; Campins, H.; Hanner, M. S.; Lederer, S. M.; Osip, D. J.; Pittichová, J.; Polomski, E. *Astrophys. J.* **2006**, *651*, 1256.
- (330) Mousis, O.; Petit, J.-M.; Wurm, G.; Krauss, O.; Alibert, Y.; Horner, J. *Astron. Astrophys.* **2007**, *466*, L9.
- (331) Wooden, D.; Desch, S.; Harker, D.; Gail, H.-P.; Keller, L. In *Protostars and Planets V*; Reipurth, B., Jewitt, D., Keil, K., Eds.; University of Arizona Press: Tucson, 2007; p 815.
- (332) Ciesla, F. J. *Meteorit. Planet. Sci.* **2009**, *44*, 1663.
- (333) Wozniakiewicz, P. J.; Bradley, J. P.; Ishii, H. A.; Brownlee, D. E.; Kearsley, A. T.; Burchell, M. J.; Price, M. C. *Astrophys. J.* **2012**, *760*, L23.
- (334) Hubbard, A.; McNally, C. P.; Mac Low, M.-M. *Astrophys. J.* **2012**, *761*, 58.
- (335) Oliveira, I.; Olofsson, J.; Pontoppidan, K. M.; van Dishoeck, E. F.; Augereau, J.-C.; Merín, B. *Astrophys. J.* **2011**, *734*, 51.
- (336) Riaz, B.; Honda, M.; Campins, H.; Micela, G.; Guarcello, M. G.; Gledhill, T.; Hough, J.; Martín, E. L. *Mon. Not. R. Astron. Soc.* **2012**, *420*, 2603.
- (337) Hughes, A. M.; Wilner, D. J.; Andrews, S. M.; Qi, C.; Hogerheijde, M. R. *Astrophys. J.* **2011**, *727*, 85.
- (338) Cyr, K. E.; Sears, W. D.; Lunine, J. I. *Icarus* **1998**, *135*, 537.
- (339) Xie, T.; Allen, M.; Langer, W. D. *Astrophys. J.* **1995**, *440*, 674.
- (340) Schräpler, R.; Henning, T. *Astrophys. J.* **2004**, *614*, 960.
- (341) Lissauer, J. J.; Stevenson, D. J. In *Protostars and Planets V*; Reipurth, B., Jewitt, D., Keil, K., Eds.; University of Arizona Press: Tucson, 2007; p 591.
- (342) Kennedy, G. M.; Kenyon, S. J. *Astrophys. J.* **2008**, *673*, 502.
- (343) Bockelée-Morvan, D. In *IAU Symposium 280*; Cernicharo, J., Bachiller, R., Eds.; Cambridge University Press: Cambridge, U.K., 2011; Vol. 280, p 261.
- (344) Drake, M. J. *Meteorit. Planet. Sci.* **2005**, *40*, 519.
- (345) Messenger, S.; Stadermann, F. J.; Floss, C.; Nittler, L. R.; Mukhopadhyay, S. *Space Sci. Rev.* **2003**, *106*, 155.
- (346) Hartogh, P.; Lis, D. C.; Bockelée-Morvan, D.; de Val-Borro, M.; Biver, N.; Küppers, M.; Emprechtinger, M.; Bergin, E. A.; Crovisier, J.; Rengel, M.; Moreno, R.; Szutowicz, S.; Blake, G. A. *Nature* **2011**, *478*, 218.
- (347) Bergin, E. A.; et al. *Astron. Astrophys.* **2010**, *521*, L33.
- (348) Teske, J. K.; Najita, J. R.; Carr, J. S.; Pascucci, I.; Apai, D.; Henning, T. *Astrophys. J.* **2011**, *734*, 27.
- (349) Banzatti, A.; Meyer, M. R.; Bruderer, S.; Geers, V.; Pascucci, I.; Lahuis, F.; Juhász, A.; Henning, T.; Ábrahám, P. *Astrophys. J.* **2012**, *745*, 90.
- (350) Elitzur, M.; de Jong, T. *Astron. Astrophys.* **1978**, *67*, 323.
- (351) Kaufman, M. J.; Neufeld, D. A. *Astrophys. J.* **1996**, *456*, 250.
- (352) Wagner, A. F.; Graff, M. M. *Astrophys. J.* **1987**, *317*, 423.
- (353) Kamp, I.; Thi, W.-F.; Meeus, G.; Woitke, P.; Pinte, C.; Meijerink, R.; Spaans, M.; Pascucci, I.; Aresu, G.; Dent, W. R. F. ArXiv e-prints 2013.
- (354) Mumma, M. J.; Weaver, H. A.; Larson, H. P. *Astron. Astrophys.* **1987**, *187*, 419.
- (355) Woodward, C. E.; Kelley, M. S.; Bockelée-Morvan, D.; Gehrz, R. D. *Astrophys. J.* **2007**, *671*, 1065.
- (356) Bockelée-Morvan, D.; Woodward, C. E.; Kelley, M. S.; Wooden, D. H. *Astrophys. J.* **2009**, *696*, 1075.
- (357) Shinnaka, Y.; Kawakita, H.; Kobayashi, H.; Boice, D. C.; Martinez, S. E. *Astrophys. J.* **2012**, *749*, 101.
- (358) Bonev, B. P.; Villanueva, G. L.; Paganini, L.; DiSanti, M. A.; Gibb, E. L.; Kean, J. V.; Meech, K. J.; Mumma, M. J. *Icarus* **2013**, *222*, 740.
- (359) Alexander, C. M. O.; Russell, S. S.; Arden, J. W.; Ash, R. D.; Grady, M. M.; Pillinger, C. T. *Meteorit. Planet. Sci.* **1998**, *33*, 603.
- (360) Clayton, R. N. *Annu. Rev. Earth Planet. Sci.* **1993**, *21*, 115.
- (361) Clayton, R. N. *Annu. Rev. Earth Planet. Sci.* **2007**, *35*, 1.
- (362) Glavin, D. P.; Aubrey, A. D.; Callahan, M. P.; Dworkin, J. P.; Elsila, J. E.; Parker, E. T.; Bada, J. L.; Jenniskens, P.; Shaddad, M. H. *Meteorit. Planet. Sci.* **2010**, *45*, 1695.
- (363) Elsila, J. E.; Charnley, S. B.; Burton, A. S.; Glavin, D. P.; Dworkin, J. P. *Meteorit. Planet. Sci.* **2012**, 201.
- (364) Elsila, J. E.; Glavin, D. P.; Dworkin, J. P. *Meteorit. Planet. Sci.* **2009**, *44*, 1323.
- (365) Pettini, M.; Cooke, R. *Mon. Not. R. Astron. Soc.* **2012**, *425*, 2477.
- (366) Linsky, J. L.; et al. *Astrophys. J.* **2006**, *647*, 1106.
- (367) Roberts, H.; Fuller, G. A.; Millar, T. J.; Hatchell, J.; Buckle, J. V. *Planet. Space Sci.* **2002**, *50*, 1173.
- (368) Bacmann, A.; Lefloch, B.; Ceccarelli, C.; Steinacker, J.; Castets, A.; Loinard, L. *Astrophys. J.* **2003**, *585*, L55.
- (369) Vastel, C.; Caselli, P.; Ceccarelli, C.; Phillips, T.; Wiedner, M. C.; Peng, R.; Houde, M.; Dominik, C. *Astrophys. J.* **2006**, *645*, 1198.

- (370) Irvine, W. M.; Schloerb, F. P.; Crovisier, J.; Fegley, B., Jr.; Mumma, M. J. In *Protostars and Planets IV*; Mannings, V., Boss, A. P., Russell, S. S., Eds.; University of Arizona Press: Tucson, 2000; p 1159.
- (371) Qi, C.; Wilner, D. J.; Aikawa, Y.; Blake, G. A.; Hogerheijde, M. R. *Astrophys. J.* **2008**, *681*, 1396.
- (372) Millar, T.-J.; Bennett, A.; Herbst, E. *Astrophys. J.* **1989**, *340*, 906.
- (373) Gerlich, D.; Herbst, E.; Roueff, E. *Planet. Space Sci.* **2002**, *50*, 1275.
- (374) Roberts, H.; Millar, T. J. *Astron. Astrophys.* **2000**, *361*, 388.
- (375) Roberts, H.; Herbst, E.; Millar, T. J. *Astrophys. J.* **2003**, *591*, L41.
- (376) Albertsson, T.; Semenov, D. A.; Vasyunin, A. I.; Henning, T.; Herbst, E. *Astrophys. J., Suppl. Ser.* **2013**, *207*, 27.
- (377) Nagaoka, A.; Watanabe, N.; Kouchi, A. *Astrophys. J., Lett.* **2005**, *624*, L29.
- (378) Watanabe, N. In *Astrochemistry: Recent Successes and Current Challenges*; Lis, D. C., Blake, G. A., Herbst, E., Eds.; IAU Symposium 231; Cambridge University Press: Cambridge, U.K., 2005; Vol. 231, p 415.
- (379) Hiraoka, K.; Mochizuki, N.; Wada, A. In *Astrochemistry—From Laboratory Studies to Astronomical Observations*; Kaiser, R. I., Bernath, P., Osamura, Y., Petrie, S., Mebel, A. M., Eds.; American Institute of Physics Conference Series; American Institute of Physics: Melville, NY, 2006; Vol. 855, p 86.
- (380) Hidaka, H.; Watanabe, N.; Kouchi, A. In *Astrochemistry—From Laboratory Studies to Astronomical Observations*; Kaiser, R. I., Bernath, P., Osamura, Y., Petrie, S., Mebel, A. M., Eds.; American Institute of Physics Conference Series; American Institute of Physics, Melville, NY, 2006; Vol. 855, p 107.
- (381) Flower, D. R.; Pineau Des Forets, G.; Walmsley, C. M. *Astron. Astrophys.* **2006**, *449*, 621.
- (382) Pagani, L.; Vastel, C.; Hugo, E.; Kokououline, V.; Greene, C. H.; Bacmann, A.; Bayet, E.; Ceccarelli, C.; Peng, R.; Schlemmer, S. *Astron. Astrophys.* **2009**, *494*, 623.
- (383) Asvany, O.; Schlemmer, S.; Gerlich, D. *Astrophys. J.* **2004**, *617*, 685.
- (384) Herbst, E.; Adams, N. G.; Smith, D.; Defrees, D. J. *Astrophys. J.* **1987**, *312*, 351.
- (385) Roueff, E.; Parise, B.; Herbst, E. *Astron. Astrophys.* **2007**, *464*, 245.
- (386) Henning, T.; Salama, F. *Science* **1998**, *282*, 2204.
- (387) Alexander, C. M. O.; Boss, A. P.; Keller, L. P.; Nuth, J. A.; Weinberger, A. In *Protostars and Planets V*; Reipurth, B., Jewitt, D., Keil, K., Eds.; University of Arizona Press: Tucson, 2007; p 801.
- (388) Tielens, A. G. G. M. *The Physics and Chemistry of the Interstellar Medium*; Cambridge University Press: Cambridge, U.K., 2010.
- (389) Schnaiter, M.; Henning, T.; Mutschke, H.; Kohn, B.; Ehbrecht, M.; Huisken, F. *Astrophys. J.* **1999**, *519*, 687.
- (390) Fitzpatrick, E. L.; Massa, D. *Astrophys. J.* **1988**, *328*, 734.
- (391) Schnaiter, M.; Mutschke, H.; Dorschner, J.; Henning, T.; Salama, F. *Astrophys. J.* **1998**, *498*, 486.
- (392) Steglich, M.; Bouwman, J.; Huisken, F.; Henning, T. *Astrophys. J.* **2011**, *742*, 2.
- (393) Duley, W. W.; Hu, A. *Astrophys. J.* **2012**, *761*, 115.
- (394) Allamandola, L. J.; Tielens, A. G. G. M.; Barker, J. R. *Astrophys. J., Suppl. Ser.* **1989**, *71*, 733.
- (395) Tielens, A. G. G. M. *Annu. Rev. Astron. Astrophys.* **2008**, *46*, 289.
- (396) Bernatowicz, T.; Fraundorf, G.; Ming, T.; Anders, E.; Wopenka, B.; Zinner, E.; Fraundorf, P. *Nature* **1987**, *330*, 728.
- (397) Henning, T.; Mutschke, H. *Spectrochim. Acta* **2001**, *57*, 815.
- (398) Matrajt, G.; Messenger, S.; Brownlee, D.; Joswiak, D. *Meteorit. Planet. Sci.* **2012**, *47*, 525.
- (399) Jessberger, E. K.; Christoforidis, A.; Kissel, J. *Nature* **1988**, *332*, 691.
- (400) Pizzarello, S.; Huang, Y. *Geochim. Cosmochim. Acta* **2005**, *69*, 599.
- (401) Caselli, P.; Ceccarelli, C. *Astron. Astrophys. Rev.* **2012**, *20*, 56.
- (402) Parise, B.; Castets, A.; Herbst, E.; Caux, E.; Ceccarelli, C.; Mukhopadhyay, I.; Tielens, A. G. G. M. *Astron. Astrophys.* **2004**, *416*, 159.
- (403) Bacmann, A.; Taquet, V.; Faure, A.; Kahane, C.; Ceccarelli, C. *Astron. Astrophys.* **2012**, *S41*, L12.
- (404) Hollis, J. M.; Jewell, P. R.; Lovas, F. J.; Remijan, A. *Astrophys. J.* **2004**, *613*, L45.
- (405) Jørgensen, J. K.; Favre, C.; Bisschop, S. E.; Bourke, T. L.; van Dishoeck, E. F.; Schmalzl, M. *Astrophys. J., Lett.* **2012**, *757*, L4.
- (406) Kahane, C.; Ceccarelli, C.; Faure, A.; Caux, E. *Astrophys. J., Lett.* **2013**, *763*, L38.
- (407) Hassel, G. E., Jr. Shock Processing of Icy Grain Mantles in Protoplanetary Disks. Ph.D. Thesis, Rensselaer Polytechnic Institute, Troy, NY, 2004.
- (408) d'Hendecourt, L. B.; Allamandola, L. J.; Baas, F.; Greenberg, J. M. *Astron. Astrophys.* **1982**, *109*, L12.
- (409) Shalabiea, O. M.; Greenberg, J. M. *Astron. Astrophys.* **1994**, *290*, 266.
- (410) Garrod, R. T.; Wakelam, V.; Herbst, E. *Astron. Astrophys.* **2007**, *467*, 1103.
- (411) Hill, H. G. M.; Nuth, J. A. *Astrobiology* **2003**, *3*, 291.
- (412) Nuth, J. A.; Berg, O. *Lunar and Planetary Institute Conference Abstracts*; Lunar and Planetary Institute: Houston, 1994; p 1011.
- (413) Kress, M. E.; Tielens, A. G. G. M.; Frenklach, M. *Adv. Space Res.* **2010**, *46*, 44.
- (414) Qi, C.; Kessler, J. E.; Koerner, D. W.; Sargent, A. I.; Blake, G. A. *Astrophys. J.* **2003**, *597*, 986.
- (415) Zasowski, G.; Kemper, F.; Watson, D. M.; Furlan, E.; Bohac, C. J.; Hull, C.; Green, J. D. *Astrophys. J.* **2009**, *694*, 459.
- (416) Garrod, R. T.; Herbst, E. *Astron. Astrophys.* **2006**, *457*, 927.
- (417) Evans, N. L.; Bennett, C. J.; Ullrich, S.; Kaiser, R. I. *Astrophys. J.* **2011**, *730*, 69.
- (418) Jones, B. M.; Bennett, C. J.; Kaiser, R. I. *Astrophys. J.* **2011**, *734*, 78.
- (419) Kim, Y. S.; Kaiser, R. I. *Astrophys. J.* **2012**, *758*, 37.
- (420) van Broekhuizen, F. A.; Keane, J. V.; Schutte, W. A. *Astron. Astrophys.* **2004**, *415*, 425.
- (421) Tideswell, D. M.; Fuller, G. A.; Millar, T. J.; Markwick, A. J. *Astron. Astrophys.* **2010**, *510*, 85.